Underwater Acoustic Imaging Devices for Portable Scour Monitoring

Terence M. Browne, P.E., M.ASCE

Collins Engineers, Inc., Phone (800) TEK-DIVE, E-mail: tbrowne@collinsengr.com

ABSTRACT

Monitoring of key infrastructure below water and the channel bottom surrounding these items is essential for ensuring public safety and promoting long-term serviceability, as well as ensuring functional reliability of these waterway structures and the waterway natural resource.

New advances in underwater acoustic imaging have emerged as a tremendous portable tool for scour monitoring. Underwater acoustic imaging can provide photo-quality visual images of submerged elements for structural inspection documentation; channel bottom elevation and material texture information for scour monitoring during flood events; spatial understanding for repair design activities; and construction observation for quality assurance documentation of scour countermeasure installations.

During hazardous flood conditions, hydrographic surveys and site evaluations by qualified underwater inspection divers to determine the maximum scour cannot always be performed due to safety reasons. When the scour depth is the deepest during a flood, this reliable portable sonar equipment can easily be used at numerous sites in an accurate, quick, and safe approach.

INTRODUCTION

The Federal Highway Administration (FHWA) requires that all highway bridges with a submerged substructure be inspected underwater to assess the structural integrity with certainty. Detecting and documenting any scour at a bridge site is a critical part of these inspections. Many owners of bridges and other infrastructure facilities are benefiting from underwater acoustic imaging by detecting and permanently capturing graphic depictions of scour depressions at a site, as well as documenting structure surface defects and erosion of submerged bank slopes.

During routine inspections as well as special scour assessments during floods, underwater acoustic imaging is now frequently used to detect and document scour so long as an inspector can access the waterway, or nearby bridge deck. If the distance from the bridge deck to the waterline is not excessive (generally considered less than ten feet), underwater acoustic imaging without other specialized equipment can be conducted from the bridge deck. Likewise, underwater acoustic imaging without a specially equipped larger vessel can be conducted from the waterway if the current is not excessive (generally considered less than 6 feet per second). For bridge deck freeboards greater than 10 feet or a waterway velocity greater than 6 feet per second, additional specialized equipment is required to deploy and maintain the sonar head in position. However, the vast majority of scour monitoring activities with underwater acoustic imaging can be conducted during a major flood by three individuals with lightweight equipment and a deployment system. Underwater acoustic imaging devices are portable, allowing data capture from any accessible area. Furthermore, data can even be obtained at some inaccessible areas caused by such conditions as debris or limited freeboard height under a bridge since the horizontal range of many sonar devices extend several hundred feet. While it is desirable to be located directly adjacent and above the imaged area to prevent shadows and distortion, useful data can still be obtained even when projecting at an angle due to obstructions.

OVERVIEW OF UNDERWATER IMAGING

Underwater imaging is a general concept that encompasses a wide variety of technologies. Underwater photography and underwater videography are the two most commonly used methods for obtaining underwater still images and underwater digital movies. However, water clarity greatly affects the quality of the images obtained by these two optical means. Furthermore, the camera range and lighting for underwater photography and videography often prohibit a large panoramic perspective, as well as only providing a two dimensional (2-D) perspective. Non-optical technologies that have demonstrated success in providing underwater images include sonar, laser, and radar. Laser scanning (often referred to as Lidar in above water applications) can produce extremely accurate underwater images, but light transmission factors related to water clarity and other limitations make it more widely used on offshore ocean structures than inland waterway bridges. Radar technologies, such as ground penetrating radar (GPR), can produce underwater images primarily of internal concrete defects or subsurface channel bottom geotechnical strata layers, while synthetic aperture radar (SAR) has been used to obtain large-area perspective underwater imaging of channel bottom topography.

Of all the non-optical underwater imaging technologies, sonar has demonstrated the most potential and is the most widely used in conjunction with scour monitoring. Even in the most turbid waters with zero visibility, sonar can provide data and images of the highest quality. Since sonar technology utilizes sound waves, it is also known as an acoustic technology. Underwater acoustic images vary in the quality resolution and dimensional perspective (2-D or 3-D) depending on the sonar device utilized. Sonar images with photo-quality resolution are referred to as high definition acoustic images. High definition acoustic images are most commonly obtained either with a 2-D perspective using sector scanning sonar, or with a 3-D perspective using multi-beam sonar. Both technologies will be discussed further in this paper.

Collins Engineers, Inc. has conducted research in conjunction with Queens University in Europe and Massachusetts DOT in the USA, to assert the usefulness of sonar technology related to bridge inspections and scour monitoring. These research studies have included comprehensive literature searches; synthesis of underwater inspection techniques nationwide as well internationally, and evaluation of data accuracy compared to diver inspections. FHWA will be conducting additional research in the United States to assess the use of sonar technology to inspect bridges especially where an underwater inspection by divers would be difficult or dangerous. FHWA will address any policy/guidance or regulatory issues regarding the use or substitution of sonar for underwater inspections by divers after their research is completed. Until then, bridge owners may use sonar technology to supplement bridge inspection diving operations (i.e., to document findings and help direct divers to areas of interest), and in situations where underwater inspections cannot be safely performed since some information is better than no information. However, sonar results alone are not currently a substitute for the data obtained by an underwater inspection performed by a qualified inspector with the appropriate intensity levels, as required by FHWA guidelines.

The *Underwater Bridge Inspection* manual published by the FHWA in 2010 outlines the various types, methods, and intensity levels associated with underwater inspections and scour monitoring. Therefore, this paper will only briefly touch on these aspects as they relate to underwater acoustic imaging, and will primarily focus on the applicability, advantages, and limitations of various sonar devices.

SONAR DEVICES

Sonar (originally an acronym for Sound Navigation and Ranging) uses transmitted and reflected underwater sound waves to detect submerged objects and measure distances. This technology is primarily used for water depth determination, underwater object detection, underwater communications, and underwater imaging. The sonar devices that are primarily used for underwater investigations are fathometers, multi-beam swath sonar, side-scan sonar, sector scanning sonar, lens-based multi-beam sonar, and sub-bottom profilers.

All sonar and radar devices operate on the simple principal of transmitting a wave toward an object to measure the time and amplitude of the reflected wave or echo. The waves are generated, emitted, and received from a transducer or antennae. The major differences between the various units are the frequency of the emitted wave, the method of focusing or directing the wave, and the display method. However, radar operates at a much higher frequency and is primarily used to evaluate subsurface observations; whereas, sonar is primarily used to obtain submerged surface data and images.

Wave frequencies can vary from sonic to radio frequencies; however, most are in the ultrasonic range. In general, low frequency waves will give lower resolution of objects but provide better penetration capabilities while the reverse is true for higher frequency waves. Most fathometers focus the waves into narrow cones of 20, 40, or 60 degrees depending on the transducer. Side-scan sonar flattens the cone into a fan shape. The scanning sonar uses a narrow beam which is progressively rotated to provide spherical coverage. The displays can vary from a single number, jagged lines, or near photographic quality depending on the amount of data gathered and processing methods used. Typically, time is converted to distance and amplitude is converted to either color or brightness. The amount of inspector interpretation is directly proportional to the quality and type of the displayed information. Therefore, it is important that the inspector understand how the unit works as well as the geometric relationship (perspective) of the transducer to the object of interest. Many times multiple perspectives make the task of display interpretation easier. The following paragraphs illustrate the various portable sonar devices that have been used for scour monitoring.

FATHOMETERS

Water depths can be manually obtained with a sounding pole or lead line, but sonar devices provide more efficient and effective retrieval of electronic data. The simplest fathometers consist of an acoustic sending/receiving device (transducer) suspended in the water and a digital or paper recording device. The paper strip-chart recorder—previously used by recreational fishermen— has long ago been adapted for use as a data collection tool for hydraulic engineers and scour inspectors due to its permanent hard-copy documentation capability. However, these inexpensive strip-chart recorders are being phased out by manufacturers and replaced by more modern survey-grade electronic precision echosounders, which work basically on the same principle and allow data collection on a digital memory card.

A fathometer works by emitting acoustic pulses through the water column toward the channel bottom by way of the transducer. The recording device measures the time it takes the pulse to reflect off the channel bottom and return to the transducer, and then converts that time into water depth. Fathometer frequencies typically range between 24 kHz and 340 kHz, with higher frequencies yielding higher resolution, but little or no channel bottom penetration. As channel bottom penetration is typically not desired when performing a fathometer survey, a higher frequency is usually used (commonly 200 kHz). Many transducers currently available offer a variable beam angle. Using a larger beam angle covers a larger area of the channel bottom; however, as it is typically desired to get the best possible reading directly below the transducer, the smallest available beam angle is usually preferred. The inspector must exercise care to avoid mistaking an exposed bridge footing that might be undermined for the channel bottom being at a higher elevation. Such an error could occur if the sound wave was returned from a beam angle that captured the water depth to the top of the footing instead of recording the deeper adjacent true channel bottom elevation within the beam. Likewise, fathometers will not provide information about the channel bottom elevation located directly below a footing and cannot provide undermining dimensions in deep voids which is only possible by a diver probing under the footing.

More advanced fathometer systems include a global positioning system (GPS) receiver or robotic total station, which require significant training and expertise. When a fathometer is coupled with one of these devices, water depths can be post-processed and referenced to a state plane or other horizontal coordinate system. This allows for very accurate channel bottom surveys, which can be easily compared to future surveys. When water conditions allow, a boat-mounted transducer allows efficient data collection. However, transducers mounted on poles, floats, or articulated arms have been used when maneuvering a boat during peak waterway flows is unfeasible.

The primary benefit of a fathometer is the ability to develop accurate channel bottom profiles. The profiles can be used to locate and quantify apparent scour depressions, areas of possible infilling, and channel bottom objects such as exposed pier footings or debris accumulation. Performing a fathometer survey prior to the diving inspection can direct the underwater inspector to potential problem areas on a bridge, as well as alert the inspector to potential below-water hazards. Overlaying and comparing channel bottom profiles from successive underwater bridge inspections can alert engineers to possible channel related problems. Bridge foundation information from as-built plans can be superimposed onto the channel cross-sections and profiles for easy reference purposes.

The primary limitation of a fathometer, or other traditional water depth sounding methods, is its inability to collect data outside the path of the vessel transporting the transducer. This limitation prevents detection of channel bottom irregularities or scour holes unless the vessel passes directly over the top of the area of interest with a narrow beam. A fathometer survey conducted during a typical underwater inspection for many state transportation agencies may include recording channel bottom profiles along the bridge fascias, as well as 100 feet and 200 feet upstream and downstream of the bridge. However, certain state DOTS, such as New York State DOT and Iowa DOT, obtain significantly more data for a highly detailed comprehensive hydrographic survey on certain waterways.

MULTI-BEAM SWATH SONAR

As mentioned previously, single beam echosounders are one of the most common forms of sonar used for scour monitoring applications. A single beam transducer is used to transmit and receive a series of sound waves to the benthic layer. The time lag between the transmission and reception is used to calculate the water depth to the point of first sound wave response. With this type of system, a single depth location is received and recorded. Single beam sonar is limited in that it does not have the ability to obtain 100 percent data coverage of the channel bottom as only one single point is returned to the transducer.

Multi-beam sonar systems, also referred to as swath echosounders, function as the name implies. This type of system uses a fanned array of sound beams that typically give 100 percent coverage of the seafloor or channel bottom. Different sound velocities and beam angles can be used to obtain required data. For instance, a typical multi-beam survey may have a fanned array that is capable of a "swath width" of seven times the water depth. This means that if the water depth is 100 ft deep, bathymetric data can be obtained up to a swath of 700 ft wide, or 350 ft to the port or starboard side of the survey vessel. The accuracy of the outer edges tapers off to the outside of the fanned array, so it is good practice to have survey track lines overlap. The accuracy of multi-beam data is quite good if the system has been calibrated and proper sensors are used. Since the direction and angle of the beams can change with the heave, pitch, and roll of the survey vessel, it is necessary to have motion compensators and a gyrocompass that account (in real-time) for this motion and relay this information back to the on board processor. Calibration checks known as "patch tests" are also performed to calibrate the sensors and account for pitch offset, roll offset, and position time delay. These tests are performed prior to the survey using the appropriate software. Calibration tests are absolutely necessary to obtain quality data.

There are many advantages of using multi-beam sonar systems. Large areas of the seafloor or channel bottom can be mapped in an efficient manner. By using multiple or overlapping passes, the hydrographic surveyor is able to obtain 100 percent bottom coverage of the area. The shape and size of underwater anomalies or obstructions can be ascertained from this data. It also has a wide range of uses that include, but are not limited to, scour area monitoring, sea floor mapping, dredging support surveys, and channel obstruction detection and identification.

SIDE-SCAN SONAR

Commercial side-scan sonar was first introduced in the early 1960s and has been successfully used for documenting underwater findings for many years. Side-scan sonar works by emitting fan-shaped acoustic pulses through the water column perpendicular to the path of the transducer. The beam is narrow in the horizontal plane (typically less than 1 degree) and wide in the vertical plane (typically between 35 and 60 degrees). The resulting images from the channel bottom and objects located on the bottom or in the water column are representative of the echoed (backscattered) target intensity within the geometric coverage of the beam. When the images are stitched together along the direction of travel, they form a continuous image of the channel bottom and objects located on the bottom or in the water column. Side-scan sonar operating frequencies usually range between 83 kHz and 800 kHz, with higher frequencies yielding better resolution, but less range. As an example, side-scan sonar with an operating frequency of 100 kHz will typically have a range of up to 1,600 feet, while side-scan sonar with an operating frequency of 800 kHz will typically have a range of less than 250 feet. The transducer is either towed behind a boat or mounted on the transom or hull of the vessel.

The primary benefit of side-scan sonar is the ability to quickly and efficiently generate detailed images of large areas of the channel bottom regardless of water clarity showing channel bottom texture (sand, cobbles, riprap, etc.) and topography. It will also detect and depict exposed underwater members (footings, seals, piles, etc.), although some interpretation is required. Side-scan sonar can be used for many purposes, including delineation of exposed sediment and geologic formations, and detection of underwater debris or structure elements.

The primary limitation of side-scan sonar is the inability to generate detailed visual images of the vertical components of submerged structures. This is true even if the towfish transducers are rotated so the beams scan vertically through the water column. As a result, scanning or multi-beam sonar are better solutions for generating simple visual images of the vertical components of submerged structures. Other limitations of side-scan sonar include the inability to detect narrow linear targets parallel to the beams; difficulty keeping the towfish at a constant location behind the vessel and at a constant elevation in the water column; keeping the vessel along a consistent line at a constant speed; and vessel pitch and roll, especially if using a hull-mounted application.

SECTOR SCANNING SONAR

The first known use of scanning sonar for a bridge assessment was performed by Collins Engineers, Inc. for the Washington DOT during the underwater inspection performed as part of the Lacey V. Murrow Floating Bridge failure investigation in 1991. Although scanning sonar was used to investigate submerged structures in the 1990s, it was not until circa 2000 that higher resolutions were available to produce photo-quality images. Since 2000, numerous bridges and waterfront facilities have been scanned to document underwater conditions, as well as monitor scour depressions located near the infrastructure. Specialized underwater engineering firms, as well as government agencies, have found purchasing a sector scanning sonar device to be the best value with a relatively economical portable equipment cost with the highest tangible "photo-quality" 2-D image resolution available.

Scanning sonar works similarly to side-scan sonar in that the transducer emits fan-shaped acoustic pulses through the water. However, unlike side-scan sonar, which requires vessel movement to develop an image, the scanning sonar device works best when it remains stationary. The acoustic images are recorded in a series of slices generated by the rotation of the transducer. Computer software stitch these slices together to form a continuous image with vertical mosaic graphics or plan-view channel bottom profiles. Scanning sonar operating frequencies usually range between 330 kHz and 2.25 MHz, with a common frequency used for channel bottom and structural imaging of 675 kHz. Although 675 kHz, which has a range of approximately 500 feet, is less than the side-scan sonar upper limit of 800 kHz, frequency is only one component of resolution. The ability to resolve a target is a combination of head stability, frequency, acoustic geometry, transducer beam width in the vertical and horizontal planes, pulse length, receiver bandwidth, signal to noise ratios, and target size, shape and acoustic impedance. As a result of the stable head, wide band width, narrow transverse beam widths, and small pulse length, images generated using scanning sonar are highly detailed even with an operating frequency of only 675 kHz.

The primary benefit of scanning sonar is the ability to produce highly detailed images of the channel bottom and vertical components of submerged structures regardless of water clarity. Scanning sonar can be used for many purposes, including detection and identification of scour depressions, areas of suspected infilling, exposed pier footings, debris accumulations, and some underwater structural deficiencies. Scanning sonar can also be used prior to and during diving operations to direct the underwater inspector to potential deficiencies and around potential below-water hazards. Near photo-quality images depicting entire or large portions of structure undermining due to scour can also be generated for inclusion into inspection reports and countermeasure design documents.

The primary limitation of scanning sonar is the inability to quickly and efficiently generate detailed images of large areas of the channel bottom. This is due to limited width range and the need for the sonar to be located close to the bottom in a stable position by way of a tripod or other deployment device for the highest quality. As a result, fathometers and multi-beam swath sonar devices are better solutions for overall channel bottom mapping of scour depressions, and side-scan sonar if searching for submerged objects over a large area in the objection. As developing highly detailed images using scanning sonar is heavily dependent on sonar positioning and stability, additional limitations may include lack of operator experience, difficult structure geometry, and excessive fast or rough waterways. Utilizing the right sonar device, or combination of sonar devices, for the exact situation and objections is critical.

So long as the acoustic image provides a clear, high definition visual of the substructure and channel bottom, many program managers feel it accomplishes a Level I inspection intensity, which allows the diving inspectors to verify any suspicious areas and focus on areas of concern, including Level II and Level III areas, as outlined by FHWA guidelines. The underwater acoustic images also provide a visual reference of the channel bottom elevations beyond hydrographic survey bathymetric contours.

LENS-BASED MULTI-BEAM SONAR

Lens-based multi-beam sonar is essentially scanning sonar that does not rotate. Scanning sonar consists of one beam that mechanically moves each transmit/receive cycle to create an image line by line. Lens-based multi-beam sonar consists of numerous beams placed side by side to create an image in one transmit/receive cycle. Many lens-based multi-beam sonar systems have manually selectable frequencies that allow for longer range for locating objects and higher resolution for investigating objects, as well as "heads-up" diver display capabilities with underwater monitor. Operating frequencies usually range between 0.7 MHz and 1.8 MHz, with higher frequencies yielding better resolution, but less range. As an example, lens-based multi-beam sonar with an operating frequency of 0.7 MHz will have lower resolution with a range of up to 240 feet, while lens-based multi-beam sonar with an operating frequency of 1.8 MHz will have higher resolution with a range of less than 50 feet.

Similar to scanning sonar, the primary benefit of lens-based multi-beam sonar is the ability to produce images of the channel bottom and submerged structures regardless of water clarity. As lens-based multi-beam sonar provides real time images, it can produce near photo-quality videos, as opposed to simply near photo-quality stills produced with scanning sonar. In addition, battery operated units with a mask-mounted display can be carried by an underwater inspector. Using such a unit, an underwater inspector can navigate to scour depressions and potential deficiencies, as well as around potential below-water hazards. The primary limitations of lens-based multi-beam sonar are range and clarity. Clarity decreases as the distance from the object increases. Also, the narrow range width makes overall observations difficult (such as evaluating large scour areas).

GEOPHYSICAL SUB-BOTTOM SONAR PROFILERS

High resolution sub-bottom profilers were first introduced in the mid-1960s and have been successfully used for defining sediment stratification and detecting bedrock. The surface component of the system generates images of the sediment stratifications, bedrock, and objects embedded in the channel bottom using either a digital or paper recording device.

The geophysical profiling systems can either be acoustic or electromagnetic radar. The electromagnetic radar system is referred to as ground penetrating radar (GPR). Radar waves are different than sonar waves. Two acoustic sub-bottom profiling systems are the tuned transducer operating between 2-15 kHz and the CHIRP color sonar operating between 200 Hz – 30 kHz.

The primary benefit of sub-bottom profilers is the ability to accurately locate sediment stratifications, bedrock, and objects embedded in the channel bottom. As a result, sub-bottom profilers are frequently used prior to marine structure construction or as part of a scour evaluation to detect infilling of depressions. With regard to underwater bridge inspection, sub-bottom profilers can be used to measure the true depth of scour depressions and locate embedded pier footings. Scour is most prevalent during a flood event; however, hazardous site conditions including complex flow patterns and the presence of drift and debris frequently prevent personnel from safely positioning instruments or diving during these events. After a flood event, the waterway current decreases and sediment is typically deposited into the scour depression. As the deposited sediment will typically consist of a different material or have a different density than the true channel bottom sediment, the sub-bottom profiler will depict the location of the previously undisturbed channel bottom.

The primary limitation of sub-bottom profilers is acoustic interference, which results in sub-bottom images that are more difficult to interpret. Acoustic interferences include multipath when operating in shallow water, and side lobes when operating near in-water structures. Multipath occurs when the transducer receives acoustic pulses that have reflected off the channel bottom, water surface, and channel bottom again. Side lobes occur when acoustic pulses encounter vertical objects, such as a bridge pier. As sub-bottom profilers use significantly lower operating frequencies than fathometers, the beam angles are typically much wider. As a result of these wider beam angles, collecting good quality sub-bottom images close to in-water structures is challenging.

CONCLUSION

Scour monitoring information can be obtained with several different techniques and displayed in a variety of documentation formats. Before the technology revolution, underwater inspectors during a site visit needed to measure individual depths by hand and manually record submerged channel bottom elevation data. Likewise, fixed methods could continuously record at one particular area on a site, but installation has proven expensive and maintenance intensive in many waterway situations. Therefore, portable sonar devices are the most commonly used method for monitoring channel bottom elevations and documenting of scour / bank erosion at site visits when deemed appropriate based on a written plan-of-action. FHWA policy requires a written plan-of-action be developed and followed for monitoring scour at all scour critical bridges and unknown foundation bridges. Figures 1 and 2 demonstrate the usefulness of underwater acoustic images.

As technology continues to improve, it is anticipated that the scour monitoring will continue to evolve with better data acquisition and display documentation. Scour that was extremely difficult to detect, or hazardous to document with divers in the past, can now be imaged to obtain measurements and photo-quality documentation. Human interaction still plays a vital part in evaluating scour depressions, and the engineer-diver's unique perspective is still needed, even with high-tech sonar devices to provide information such as channel bottom firmness, probe rod penetration data, and details on undermining beneath a foundation.

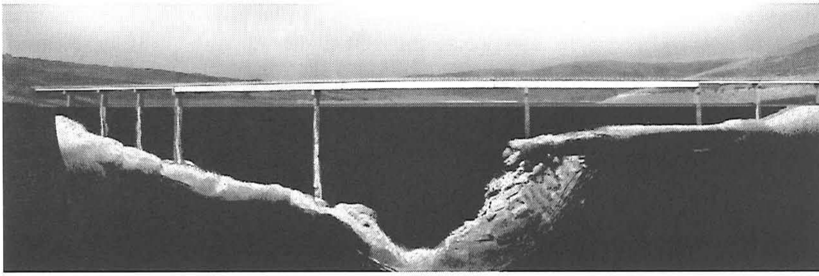

Figure 1: Scanning Sonar Image of Bridge Fascia and Channel Cross-Section.

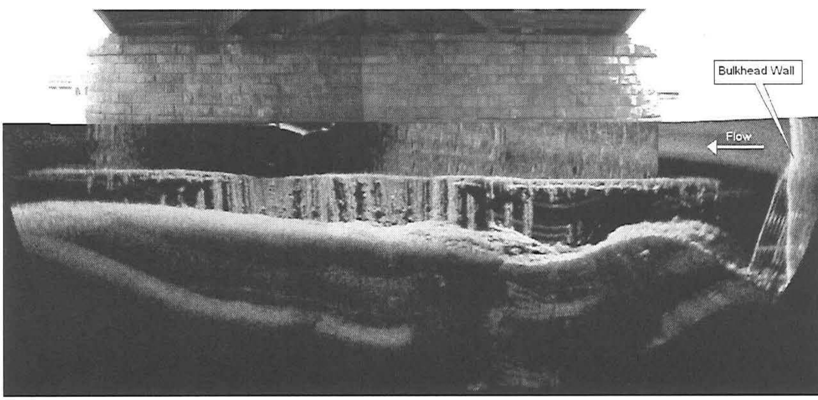

Figure 2: Scanning Sonar Image of Bridge Pier and Channel Bottom with Scour.

REFERENCES:

Browne, T., "Improvement of Underwater Bridge Inspection Documentation with Innovative Sonar Technology," FHWA Bridge Engineering Conference, 2010.

Browne, T. and Strock T., "Overview and Comparison of Nationwide Underwater Bridge Inspection Practices," TRB No. 2108 – Maintenance and Management of the Infrastructure, *Journal of the Transportation Research Board*, 2009.

Federal Highway Administration, Atlanta Technical Resource Center Memo by Cynthia Nurmi, 2009.

Federal Highway Administration, *Underwater Bridge Inspection Manual*, Publication No. FHWA-NHI-10-026, 2010.

Monitoring Bridge Scour by Bragg Grating Array

S. Manzoni[1], G. Crotti[2], A. Cigada[3], F. Inzoli[4] and F. Ballio[5]

[1] Assistant professor, Politecnico di Milano, Dept. of Mechanics – Via La Masa 1, 20156 Milan (Italy); PH (+39) 0223998589; e-mail: stefano.manzoni@polimi.it
[2] Engineer, Politecnico di Milano, D.I.I.A.R. – Piazza Leonardo da Vinci 32, 20133 Milan (Italy) PH (+39) 0223996234; e-mail: gianluca.crotti@polimi.it
[3] Professor, Politecnico di Milano, Dept. of Mechanics – Via La Masa 1, 20156 Milan (Italy); PH (+39) 0223998487; e-mail: alfredo.cigada@polimi.it
[4] Professor, Politecnico di Milano, Dept. of Energy – Via Lambruschini 4, 20156 Milan (Italy) PH (+39) 0223993883; e-mail: fabio.inzoli@polimi.it
[5] Professor, Politecnico di Milano, D.I.I.A.R. – Piazza Leonardo da Vinci 32, 20133 Milan (Italy) PH (+39) 0223996236; e-mail: francesco.ballio@polimi.it

ABSTRACT

A new real time monitoring system for river bed elevation is presented. The instrument is based on optical fiber technology. With this device it is possible to reduce uncertainties in risk evaluations during flood events, especially those related to identification of bridges in critical scour condition. The working principle is explained and experimental tests are discussed. Device is presently ready for field application.

Introduction

Scour around bridge piers and abutments is one of the major causes for bridge failure (Richardson et al., 1993; Melville, 1992; Melville and Coleman, 2000). Real time monitoring of scour depths is a crucial tool to reduce uncertainties in evaluating risk at bridges during flood events. In spite of a relatively wide variety of possible technologies, no one can be considered to be a consolidated standard, as all methods (among them, echo sounders) present significant drawbacks, particularly during flood conditions (NCHRP, 1997).

The paper presents an innovative method to measure real-time scour depths around river bridge structures under both ordinary and flood conditions. The new approach (Cigada et al., 2008) adopts an array of temperature sensors based on optical fiber technology (Fiber Bragg Grating). Fiber is heated by an electrical circuit thanks to the Joule effect. This device measures temperature gradient to define in which environment every sensor is immersed; then it is possible determine the interface between water and sediments, that is the level of the river bed.

Presentation of the new device includes technical information about the instrument and the technology used. Moreover some laboratory tests are shown and discussed to evaluate the effectiveness and reliability of the technique.

Basic concepts of fiber Bragg grating

The fiber Bragg grating (FBG in the following) is a specific wavelength reflector (Hill et al., 1997) built up into the fiber core. More than one Bragg grating can be placed in the same fiber. The fiber is connected to sensing interrogation system that beams light within the fiber and receives reflected wavelengths. When light reaches the grating, a particular wavelength is reflected, while the others pass through it (Figure 1); the reflected wavelength depends on the geometrical features of the Bragg gratings (Hill et al., 1997). If in a fiber there is more than one Bragg grating, every FBG has a particular and different spectrum.

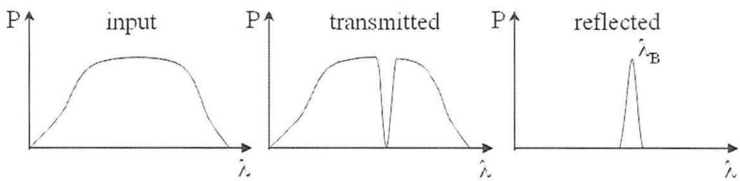

Figure 1. P is power, λ is the wavelength and λ_B is the reflected wavelength.

Literature (James et al., 1996) shows how the reflected wavelength shifts when the Bragg grating undergoes a mechanical strain and/or a temperature change (Figure 2), so that FBGs are commonly used for strain and temperature measurements.

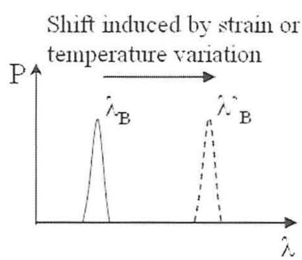

Figure 2. λ_B is the reflected wavelength at initial condition; λ'_B is the reflected wavelength after the shift.

The Bragg wavelength shift $\Delta\lambda$ due to a temperature change ΔT and a mechanical strain ε is:

$$\frac{\Delta\lambda}{\lambda_B} = k_g \cdot (\varepsilon_m + \varepsilon_t) + \alpha_r \cdot \Delta T = k_g \cdot (\varepsilon_m + \alpha_{sp} \cdot \Delta T) + \alpha_r \cdot \Delta T \tag{1}$$

where λ_B is the Bragg wavelength at the starting condition, k_g is the gage factor and α_r is the change of the refraction index per unit of temperature. The first term on the right side describes the strain impact caused by force (ε_m) and temperature (ε_t), while the second term gives the effect of a temperature change on the refractive index of glass (glass constitutes the outer part of the fiber). Finally, the strain due to temperature variation can be expressed as $\varepsilon_t = \alpha_{sp}\ \Delta T$, where α_{sp} is the linear thermal expansion coefficient of the specimen.

For the present application, FBGs are used for solely temperature measurements. It is therefore necessary to make the response of each sensor non-dependent on possible mechanical strain of the fiber. In this case the fiber is embedded into a stainless steel tube (3 mm of diameter) abounded with thermal gel. Preliminary tests have proved that the FBG sensor, in this configuration, does not sense any mechanical strain ($\varepsilon_m = 0$). Equation (1) thus becomes:

$$\frac{\Delta\lambda}{\lambda_B} = \left(k_g \cdot \alpha_{sp} + \alpha_r\right) \cdot \Delta T \tag{2}$$

Once all the parameters of equation (2) are known, ΔT values are obtained by measurements of $\Delta\lambda$ along the fiber.

Device set up

The FBGs into a fiber measure temperature of the environment. This array is set up in vertical position, just close to the pier (Figure 3 shows system layout). In this configuration some sensors are exposed to flowing water and the rest of FBGs are buried in the bed.

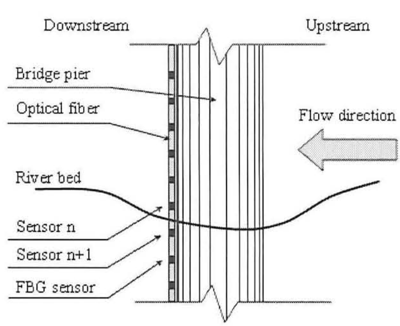

Figure 3. System layout.

Outside the steel tube that contains the fiber there is an electrical circuit connected to the power unit (Figure 4). When the power unit is turned on, the constant heat flux produced by the Joule effect is scattered due to conduction in the bed and convection in the flowing water. Heat dispersion is much higher in flowing water; therefore, the sensors exposed to flowing water sense a lower temperature increment than those buried in the bed when the electric circuit is switched on.

The measurement resolution depends on the distance between consecutive sensors. If one assumes that under ordinary conditions the bed level is defined by sensors n and n+1 (Figure 3), during a flood event the local scour around bridge pier changes the bed level and sensor n+1 (Figure 3) becomes exposed to flowing water. This changing decrease the different heat dispersion sensed by that FBG, which starts sensing a lower temperature increment respect to the previous condition. In this case the new bed level is defined by sensors n+1 and n+2. This measurement device can always determine the level of the river bottom, whatever flow conditions are considered.

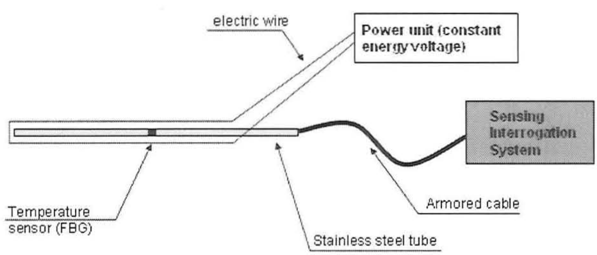

Figure 4. Electric wire configuration.

Figure 5 shows the final configuration for the laboratory scale device used in the tests. Three electric wires were wrapped along the steel tube. The contact between tube and electrical circuit is guarantee by heat-shrinking. Notice that a field-scale sensor would have the same dimensions.

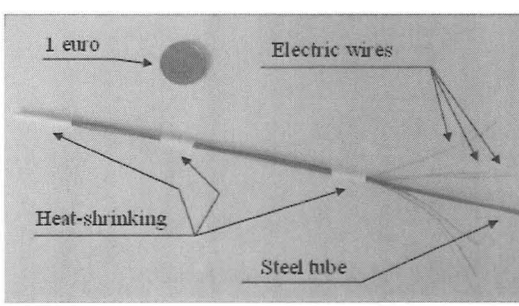

Figure 5. Main device components. In the final configuration the heat-shrinking covers the whole fiber.

Laboratory tests

The tests have been performed in the laboratory of Hydraulics at the Politecnico di Milano, Milan, Italy. The water channel had base and height of 100 and 70 cm, respectively. The water level was 60 cm and the average velocity of the flow was 0,4 m/s. The fiber was attached to a cylinder that simulated a pier. This layout allowed to test temperature sensors immersed in flowing water (Figure 6a).

To simulate the sensors buried in bed an external cylinder was added (with a larger diameter respect to the previous cylinder). The space between them was filled up with sediments and saturated with water (Figure 6b).

For both configurations the main characteristics of all tests are: dissipated power 0→50,5 W/m and data collected for longer than 100 seconds.

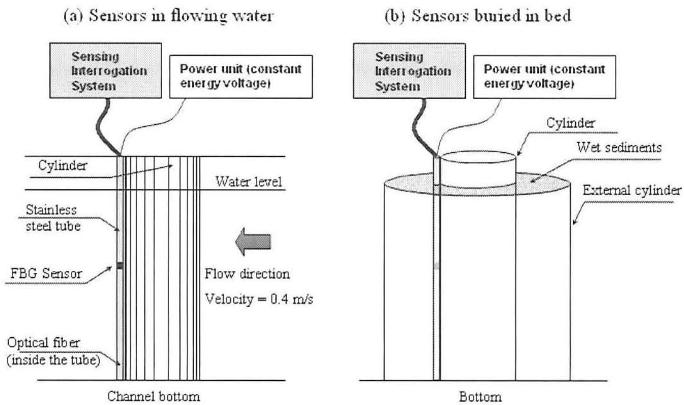

Figure 6. Layout of laboratory tests.

Figure 7 presents a typical response of the sensors in the two different environments: flowing water and buried in bed (wet sediments). Before t = 0 s, the power unit is off and the sensor measures the temperature of the environment. When the power unit is turned on, the measured temperature value increases. Heat is dissipated by conduction in the bed and convection in the flowing water. For both situations the response of the sensors shows an initial transient where the constant generated heat flux is higher than the flux scattered in the environment, and the temperature measured by the sensor increases. After the transitory, an approximately stable condition is reached.

The difference ΔT between the equilibrium and the initial temperature can be used to distinguish among sensors in different conditions (i.e., facing flowing fluid or saturated soil). The increase of (equilibrium) temperature due to heat dissipation, ΔT, is always larger in the soil than in the flowing water. However the power of heat generation highly influences the reliability of the measure. In fact an increase of dissipated power goes along with an increase of temperature variation (Figure 7). The relationship between the dissipated power and the temperature variation

(Δtemperature) is approximately linear for both the environments in which the sensor is immersed; in flowing water the proportionality coefficient is smaller than that for the soil. As a consequence, sensors exposed to the different environments can be distinguished in spite of the unavoidable local disturbances, given that the heating power is large enough. For the tested configuration, figure 8 shows that a dissipated power larger than 10-15W/m is sufficient to robustly detect the two different behaviours.

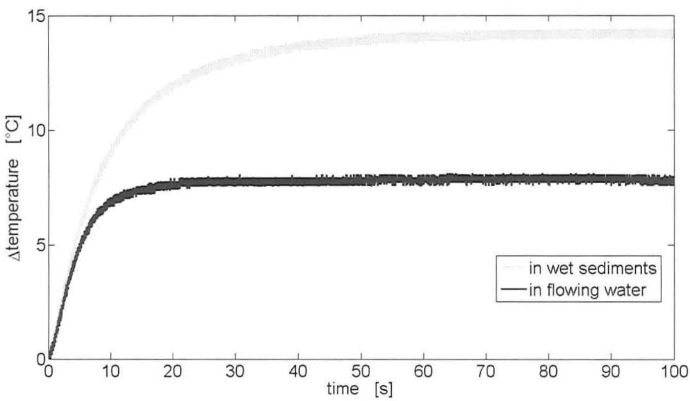

Figure 7. Response of the FBG in flowing water (black line) and in wet sediments (gray line). The constant dissipated power per meter of fiber was 50.5 W/m.

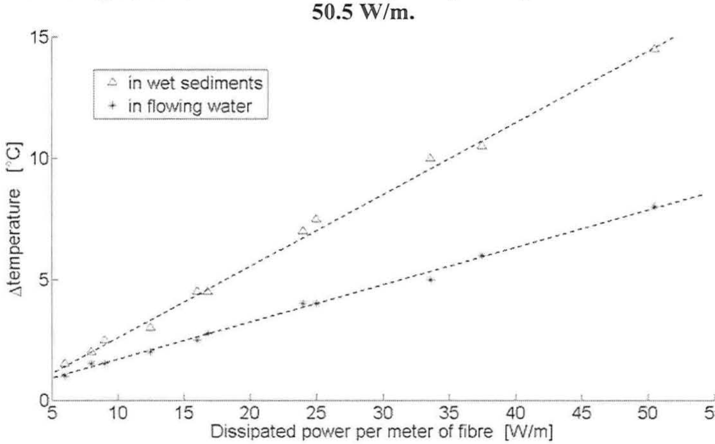

Figure 8. Δtemperature (steady state temperature – starting temperature) (ΔT in equation 1) as a function of the dissipated power in Watt per meter of fiber. The sensor is that already considered in Figure 7.

As an alternative to the temperature increase ΔT, proper time constant could be used to distinguish sensors immersed in the two environments. In fact, time histories for temperatures can be approximated as:

$$T = \Delta T\left(1 - e^{-T/\tau}\right) + TS \tag{3}$$

where ΔT was already defined as the difference between the steady-state temperature and the starting temperature, TS is the starting temperature and τ is the time constant.

The response of sensors in the two environments is different in term of time constant. Figure 9 shows that time constants have little (if any) dependence on the dissipated power, being equal to about 10 seconds for wet sediments and about 5 seconds for flowing water condition.

The time constant of wet sediments is always higher than the flowing water condition for any dissipated power (Figure 10). This result allows to consider the time constant τ as an additional parameter. In fact it is possible define the bed level estimating the time constant for all the sensors.

The comparison between figures 8 and 9 clearly shows that the combined used of the time different ΔT and the time constant τ allow to discriminate between the two environments for any value of the dissipated power.

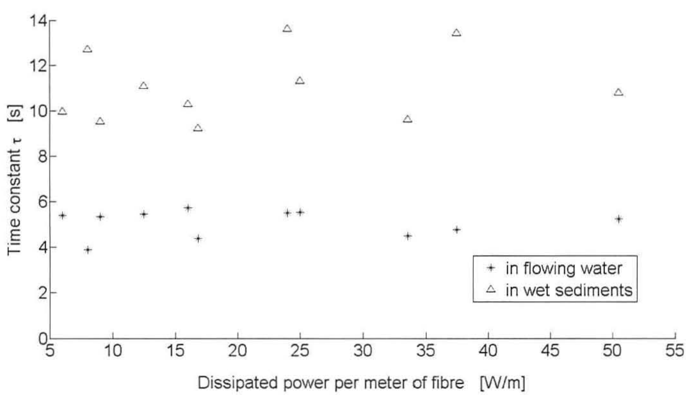

Figure 9. Time constant τ as a function of the dissipated power in Watt per meter of fiber.

Conclusion

In this work a device for scour measurement has been tested. The device is a sedimenter composed by an array of temperature sensors based on optical fiber technology (Bragg gratings). Fibers are heated by an electrical circuit and the sediment/water interface is detected by means of the different thermal behaviour of the system in two environments. Both the temperature increase due to the heating and time constant of transients can be used as indicators, as they are both larger for sensors buried in the bed than those for sensors in flowing water. The position of the bed is identified by two consecutive sensors showing different thermal behaviours. The combined use of both indicators allows for reliable detection of the bed level.

Laboratory tests have proved that the response of the instrument is satisfactory. The instrument can find out the bed level independently of flow condition of the river. Even if other tests are in progress to improve the instrument efficiency the first experimental installation will be ready in few months near Borgoforte, in the Po River, Italy.

Acknowledgements

We acknowledge with gratitude Dr. Alessio Radice of Politecnico di Milano, Dept. of Hydraulics, Milan, Italy, for comments on the first version of the manuscript.

References

Cigada A., Ballio F., Inzoli F. (2008). Hydraulic Monitoring Unit, application for international patent n. PCT/EP2008/059075.

Hill K.O., Meltz G., Fiber Bragg grating technology fundamentals and overview. Journal of Lightwave Technology 15(8) (1997) 1263-1276.

James S.W., Dockney M.L., Tatam R.P., "Simultaneous independent temperature and strain measurement using in-fibre Bragg grating sensors". Electronics Letters 32(12) (1996) 1133-1134.

Melville B.W. (1992) "Local scour at bridge abutments", J. Hydraul. Eng. 118(4), pp. 615-631.

Melville B.W. and Coleman S.E (2000) "Bridge scour", Water Resources Publications, LLC, Highlands Ranch, Colo.

National Cooperative Highway Research Program (NCHRP) "Report 396: Instrumentation for Measuring Scour at Bridge Piers and Abutment", 1997.

Richardson E.V., Harrison L.J., Richardson J.R. and Davies S.R. (1993) "Evaluating scour at bridges", publ. FHWA-IP-90-017, Federal Highway Administration, US Department of transportation, Washington DC.

Bridge Scour Monitoring Technologies: Development of Evaluation and Selection Protocols for Application on River Bridges in Minnesota

M. Lueker[1], J. Marr[2], C. Ellis[3], A. Hendrickson[4], and V.Winsted[5]

[1]St. Anthony Falls Laboratory, Department of Civil Engineering, University of Minnesota, 2 3rd Ave. SE, Minneapolis, MN, 55413; PH (612) 626-3058; e-mail: luek0004@umn.edu
[2]St. Anthony Falls Laboratory, PH (612) 624-4427; e-mail: jmarr@umn.edu
[3]St. Anthony Falls Laboratory, PH (612) 624-4447; e-mail: ellis05@umn.edu
[4]Bridge Office, Minnesota Department of Transportation, 3485 Hadley Avenue North, Oakdale, MN 55128; PH (651) 366-4466; e-mail: andrea.hendrickson@dot.state.mn.us
[5]Department of Electrical & Computer Engineering and Technology, Minnesota State University-Mankato, 137 Trafton Science Center S, Mankato, MN 56001; email: vincent.winstead@mnsu.edu

ABSTRACT

Bridge failure can result from scour of riverbed sediment near bridge abutments or piers. Fixed scour monitoring technologies provide a viable countermeasure option for measuring scour depth and alerting the appropriate personnel. Several fixed methods of monitoring bridge scour have been developed. To help the Minnesota Department of Transportation select the most appropriate instrument given site-specific bridge and stream conditions, the Scour Monitoring Decision Framework (SMDF) was developed. This selection tool is a macro-enabled Excel workbook that assists personnel with evaluation and selection of available fixed scour monitoring technologies for a specific bridge and stream. The user enters site-specific bridge and stream characteristics that are compared to instrument characteristics and results are presented in a percentage type score for each type of available instrument within the SMDF database.

INTRODUCTION

Streams at waterway bridges present significant challenges for hydraulic engineers. They create highly variable situations and can damage bridge structures in numerous ways. Broadly, these mechanisms involve scour and stream instability. Scour is the erosion of bed material due to either bridge foundations located in the stream flow, or channel constriction at bridge sites. Alternatively, stream instability involves the lateral or vertical movement of a stream over long time periods. According to the National Cooperative Highway Research Program (NCHRP) Report 396, *Instrumentation for Measuring Scour at Bridge Piers and Abutment*, (Lagasse et al, 1997, p. 4), these stream-related issues account for 60% of bridge failures in the United States. Countermeasures to mitigate these issues usually involve physical protection, such as riprap, and/or monitoring. In cases where physical countermeasures are cost prohibitive, monitoring may be used as an acceptable alternative. Monitoring can be further subdivided into portable monitoring or fixed monitoring. Portable monitoring involves manually measuring stream bed elevations at structures, whereas fixed monitoring involves the deployment of a device to record scour depths that are later retrieved or sent electronically to the appropriate personnel. The goal of this work is to aid bridge engineers with proper selection of the numerous fixed scour monitoring instruments available.

The final product of this work is the Scour Monitoring Decision Framework (SMDF). This decision-making tool addresses one of the major problems with regard to fixed scour monitoring instrumentation. NCHRP Report 396 best describes the issue: "no *single* methodology or instrument for measuring scour at bridge piers and abutments can be used to solve the scour measuring problems for *all* situations encountered in the field" (p. 84). The report further describes guidance for selection of appropriate monitoring instrumentation as an area for future research. The SMDF is a Visual Basic for Applications (VBA) enabled Excel workbook that accepts site-specific information one bridge site at a time. This information includes details on bridge, stream, and scour, and then compares the information to critical characteristics for fixed scour monitoring equipment. The output is a list ranking the instruments in the SMDF and an overview of how the characteristics affect the score for each instrument. After entering the required information, the user has a good familiarity with the site and, along with the output of the SMDF, can more confidently select the instrument(s) best suited for the site.

METHODOLOGY

Gathering information for construction of the SMDF included the following:

- Literature review
- Previous installation assessments
- Bridge/stream/scour characterization
- Fixed scour monitoring instrumentation characterization

The literature review included documents on overall bridge scour, specific instruments, and implementation. One of the greatest problems with fixed scour monitoring identified in the literature was the ongoing maintenance required. The majority of the successful long-term deployments were affiliated with research projects that allowed continual attention to the system. Most other deployments that did not allocate funds for ongoing maintenance failed soon after installation. Another major problem identified in the literature review was major damage to systems from impacts with woody debris carried by the stream.

The assessment of previously installed fixed scour monitoring deployments included all those in Minnesota and significant installations in the rest of the United States. These assessments agree with the above conclusions found in the literature review involving maintenance and susceptibility to river debris.

Bridge/stream/scour (site) characterization

The bridge/stream/scour characterization was organized and designed to utilize information readily available at the Minnesota Department of Transportation (Mn/DOT). These sources of information include bridge plans and scour calculations. This investigation balancing the bridge/stream/scour characterization and readily available information to the DOT resulted in the required SMDF inputs listed in the following tables. They are broken down into bridge conditions (Table 1), stream conditions (Table 2), and scour conditions (Table 3). This information is either directly input into the SMDF by the user or is extracted from other information the user inputs.

Table 1. Bridge conditions used as SMDF inputs

Deck	Foundation	Other
Pedestrian Path	Pier/Abutment Type	Distance to Responsible Office
Ease of Lane Closure	Foundation Extension Past Pier Face	Distance to Populations
Deck Height above Typical Bed	Angle of Attack / Embankment Angle	Average Daily Traffic
Deck Extension Past Pier Face		Available Power Sources
		Available Telemetry
		Time until Bridge Replacement

Table 2. Stream conditions used as SMDF inputs

Local Hydraulics	Stream Morphology	Debris
Approach Velocity	River Type, i.e. stable, meandering	History of Debris
Overtopping Bridge	Flow Habit, i.e. perennial, flashy	Channel/Floodplain Ratio
Typical Water Depth	Lateral Migration	Frequency of Overbank Flooding
Significant Entrained Air	Vertical Migration	Debris Sources Upstream
Significant Entrained Solids	Upstream Tributary	
	Downstream Mainstem	

Table 3. Scour conditions used as SMDF inputs

Bed Material	Scour Characterization
Surface Material Type	Scour Depth
Subsurface Material Type	
Cobbles/Other Buried Structure	
Countermeasure Types	
Countermeasure Conditions	

These bridge/stream/scour conditions are expanded further to the point where they can be defined by a boolean value indicating if each characteristic describes the bridge site or not. For example, "Countermeasure Types" is further divided into None, Riprap, and/or Concrete.

Fixed scour monitoring instrumentation characterization

The characterization of fixed scour monitoring devices resulted in the 24 critical characteristics listed in Table 4. These were selected to be as broad as possible to make them applicable to both current instruments and, hopefully, instruments developed in the future. This allows comparison between new instruments and those currently used within the framework. The characteristics are defined such that they are all positive. This simplifies scoring in the SMDF and results in no negative scoring for each instrument characteristic.

Table 4. Critical fixed scour monitoring attributes

Indirect Measurement	Resistant to Ultraviolet Radiation
Continuous Spatial Measurement	Insensitive to Aerated Flow
Measures Current Bed Level	Vandal Resistant
Long Measurement Range (> 10 Feet)	Datalogger Compatibility with Sensor
Correct Operation Validation	Wireless Sensor Connection
Sensor Not Exposed to Ice/Debris	Water/Air Jet Not Required for Installation
Sensor Resistant to Ice/Debris Damage	Pile Driver Not Required for Installation
Sensor Insensitive to Entrained Material	Auger Not Required for Installation
No Moving Parts	Long System Lifespan
Free Standing Device	Heavy Equipment Not Required for Sensor Maintenance
Vibration Failure Resistant	Equipment Simplicity
Corrosion Resistant	Foundation Settling Not Required

The first step in the SMDF selection process involves determining the importance of each of these instrument characteristics for the bridge location currently of interest. This utilizes a matrix of weighted values comparing the relation of each site characteristic to each instrument characteristic. If an instrument characteristic is not affected by a given site characteristic, the weighting value for that relationship is zero. As stated before, the site characteristics are expanded to the point where the site is defined by boolean values. These boolean values essentially turn on of off the individual weighting affiliated with each site characteristic with regard to each instrument characteristic. At the end of this process, the applicable weighting values for the each instrument characteristic are summed. Thus, the importance of each instrument characteristic is determined.

Instrument selection

The second and final step in the SMDF selection process involves selecting the most appropriate instrument given the totaled instrument characteristic scores. This uses a second matrix of boolean values indicating which instrument characteristics defines each instrument. Table 5 lists the fixed scour monitoring instrument types currently in the SMDF and shows which instrument characteristics describe each instrument. During computation, the associated summed instrument characteristic score calculated in the previous step replaces each "1" in the instrument row. The total for each instrument is summed and a score is given. The last instrument is the "Ideal Instrument" which is described by all of the positive characteristics and therefore has the highest score. To provide some dimension to the score calculated for the other instruments, each of them are divided by the "Ideal Instrument" score resulting in a percentage type score.

Additional instruments may be added to the SMDF by determining what instrument characteristics define the new instrument and adding them to the appropriate worksheets is the SMDF Excel workbook.

Table 5. Instruments and satisfied instrument attributes used in the SMDF

	Indirect Measurement	Continuous Measurement	Measures Current Bed Level	Long Measurement Range (> 10 Feet)	Correct Operation Validation	Sensor Not Exposed to Ice/Debris	Sensor Resistant to Ice/Debris Damage	Sensor Insensitive to Entrained Material	No Moving Parts	Free Standing Device	Vibration Failure Resistant	Corrosion Resistant	Resistant to UltraViolet Radiation	Insensitive to Aerated Flow	Vandal Resistant	Datalogger Compatibility with Sensor	Wireless Sensor Connection	Water/Air Jet Not Required for Installation	Pile Driver Not Required for Installation	Auger Not Required for Installation	Long System Lifespan	Heavy Equipment Not Required for Sensor Maintainence	Equipment Simplicity	Foundation Settling Not Required
Sonar	1	1	1	1	1				1		1	1				1		1	1	1			1	1
Manual Sliding Collar				1	1			1				1	1	1				1		1	1		1	1
Automatic Sliding Collar				1	1	1		1		1		1	1	1	1	1		1		1	1		1	1
Float-Out				1		1	1	1	1	1	1	1	1	1	1	1	1	1	1					1
Tilt Angle/Vibration Sensors	1				1	1		1	1		1	1		1		1	1	1	1	1		1		
Sounding Rods		1			1			1					1	1				1	1	1	1	1	1	1
Piezoelectric Film			1		1	1		1		1				1	1	1			1	1		1		1
Time Domain Reflectometry		1	1		1	1			1	1					1	1			1	1		1		1
PSDS			1	1	1		1		1									1		1		1	1	1
Ideal Instrument	1	1	1	1	1	1	1	1	1	1	1	1	1	1	1	1	1	1	1	1	1	1	1	1

SMDF OUTPUTS

The main output of the SMDF is a listing of the percentage type scores for each instrument. In addition to this score, the anticipated cost of the instrument without datalogger or telemetry devices is provided. The datalogger and telemetry are seen as fixed costs. Figure 1 shows a portion of a screenshot of the output of the SMDF for Bridge 07038 in southern Minnesota.

Pier 1	**Pier 1**		
Sensor Type	**Score (Percent)**	**Score (Cost)**	
Sonar	75	\$6000 + Datalogger	<<< Sensor Selected
Float-Out	73	\$2000 + Datalogger	
Time Domain Reflectometry	70	\$3,650 + Datalogger	
PSDS	67	? + Datalogger	
Piezoelectric Film	67	\$1000 + Datalogger	
Automatic Sliding Collar	67	\$4100 + Datalogger	
Sounding Rods	66	\$7,000	
Manual Sliding Collar	57	\$2,500	
Tilt Angle/Vibration Sensors	52	\$500 + Datalogger	
Warning ------>	Angle of Attack	Greater Than 10 Degrees	
Warning ------>	Local Curvature	Greater Than 30 degrees	

Figure 1. SMDF Results for Pier 1 of Minnesota Bridge 07038

In addition to helping users select the most appropriate instrumentation for a given bridge site, warnings are also provided which indicate the potential for atypical scour at a foundation. Here, typical scour is assumed to occur directly in front of piers and at the upstream portions of abutments. The purpose of the warnings is to inform the user of potentially complex scour and indicate additional information is needed to make sure the instrument measures the location of deepest scour and/or most susceptible portion(s) of the bridge structure. Warnings are output for the following anticipated scenarios at a bridge site:

- Angle of attack greater than 10°
- Stream overtops bridge deck
- Upstream tributary within five main channel widths
- Downstream mainstem within two main channel widths
- Local stream curvature greater than 10° using stream cross-sections two main channel widths upstream and downstream
- Local stream curvature greater than 30° using stream cross-sections two main channel widths upstream and downstream
- Surface bed material is clay
- Subsurface bed material is clay

An example of these output warnings are shown at the bottom of Figure 1. The effect of these conditions on scour depth and location are out of the scope of the SMDF. It is the responsibility of the user to further investigate the issues related to these warnings.

After reviewing the percentage type scores, the SMDF allows the user to select an instrument available in the SMDF. A bar graph for each entered foundation shows the importance of each instrument characteristic; this is indicated as "Ideal Instrument" in the legend. If the user has made an instrument selection, the graph also shows whether the selected instrument satisfies each instrument characteristic. Figure 2 shows an example output of this bar graph produced. The information on the graph illustrates the weaknesses of the selected instrument. Appendices of the associated user manual provide information on potential mitigation techniques for each instrument characteristic unsatisfied by the selected instrument.

The user manual also defines all of the inputs for the SMDF and additional general information on the critical instrument characteristics, user inputs. More information on each available technology is also included in the SMDF.

The last output of the SMDF summarizes the inputs to allow users to quickly review this information and find any erroneous inputted data.

SMDF DEMONSTRATION

The SMDF was applied to five demonstration sites in Minnesota. These sites ranged from a two-lane single-span bridge to an interstate bridge and provided a wide range of situations to test the SMDF. All of the bridges selected have a high likelihood of scour. The results presented by the SMDF matched well with intuitive results, and the framework successfully conveys site-specific issues to the user through its output.

Work plans were developed for two of the demonstration sites. This portion of the project illustrated the next steps if deployment of a site is further investigated. The work plans included example drawings of equipment installation, items required for installation, and pricing. The total cost for each of the two installations was estimated to be \$30,100 and \$37,100. Both work plans involved installation of two sonar

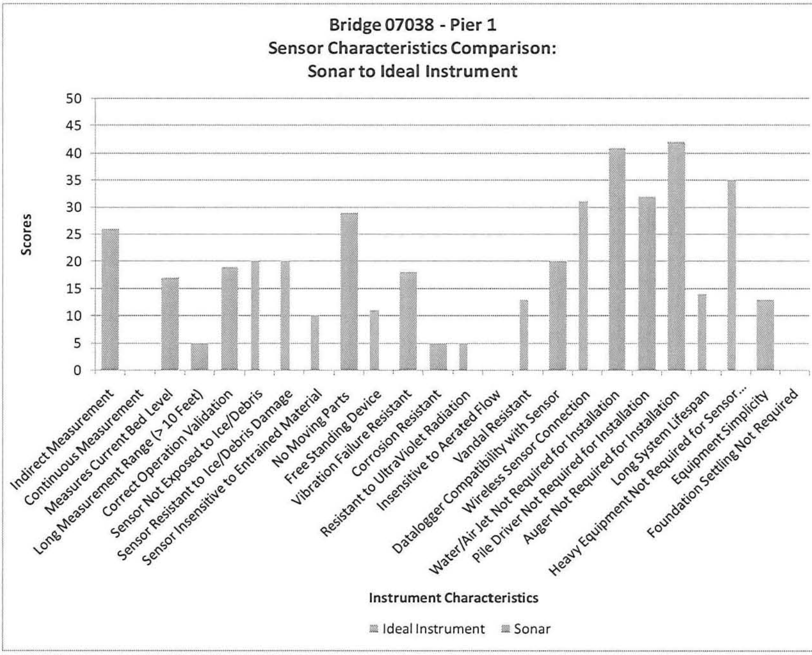

Figure 2. SMDF Bar Graph Results for Pier 1 of Minnesota Bridge 07038

devices, each monitoring a single pier. The more expensive installation included float-out devices for monitoring an abutment. These costs included significant labor costs associated with personnel hours for initial sensor setup and programming. The installation costs match well with other estimates for these types of instruments. Yearly maintenance was estimated to be $2,200. The first year likely will incur more costs as unforeseen issues with the installations are resolved.

CONCLUSIONS

In conclusion, the Scour Monitoring Decision Framework should help engineers when selecting or investigating the possibility of using fixed scour monitoring on a specific bridge site. The engineers should gain insight into site-specific issues for each bridge from both the output of the framework as well as the process of entering the necessary input. The results are intuitive and determine the most critical bridge/stream/scour characteristics for each site. In addition, the SMDF provides warnings for situations where atypical scour is likely to occur, i.e., high angle of attack of the stream on the pier.

The programmers defined the weighting values, used to relate the importance of bridge/stream/scour characteristics to instrument characteristics, to achieve the desired output after careful examination of five demonstration bridges. These values are critical to the instrument selection and are the largest source of potential error in the SMDF selection.

During application of the SMDF to the demonstration sites, the most common highest-rated instrument for monitoring piers were sonar devices and the most common highest-rated instrument for monitoring abutments were float-out devices.

Recommendations for future research for Mn/DOT include the following four items:

- Additional deployments: Future deployments will provide the best information on difficulties that arise with fixed scour monitoring deployments.
- Collaboration with researchers: Installations that were part of a larger research effort were found to be the most successful in the literature review. Finding other parties interested in field-scale scour studies will help ensure good initial and continued deployments.
- Additional research into individual sensors: Some instruments have not been widely used, so additional research focusing on these individual instruments may be beneficial. New instruments are continuously being developed; two examples are tethered float-outs and time domain reflectometry devices.
- Database management: Database management is crucial to the success of deployment over the long term. Along with telemetry, a good database can provide long-term trends, near instantaneous readings, and automated error checking.

ADDITIONAL INFORMATION

The full report on this work, *Bridge Scour Monitoring Technologies: Development of Evaluation and Selection Protocols for Application on River Bridges in Minnesota*, and Scour Monitoring Decision Framework Microsoft Excel workbook can be found on the University of Minnesota, Center for Transportation Studies website at http://www.cts.umn.edu/Publications/ResearchReports/reportdetail.html?id=1916.

REFERENCES

Minnesota Department of Transportation, 2008, *Bridge Inspection Manual Version 1.7*, (Internal document).

Hunt, B., 2009. *Monitoring Scour Critical Bridges*. NCHRP Synthesis 396, Transportation Research Board, Washington, D.C.

Lagasse, P.F., E.V. Richardson, J.D. Schall, and G.R. Price, 1997. *Instrumentation for Monitoring Scour at Bridges*. NCHRP Report 396, Transportation Research Board, National Research Council, National Academy Press, Washington, D.C.

Lagasse, P.F., J.D. Schall, and E.V. Richardson, 2001a. *Stream Stability at Highway Structure. Hydraulic Engineering Circular 20,* Third Edition, FHWA NHI 01-002, Federal Highway Administration, U.S. Department of Transportation, Washington, D.C.

Lagasse, P.F., L.W. Zevenbergen, J.D. Schall, P.E. Clopper, 2001b. *Bridge Scour and Stream Instability Countermeasures – Experience, Selection, and Design Guidance. Hydraulic Engineering Circular 23*, Second Edition, FHWA NHI

01-003, Federal Highway Administration, U.S. Department of Transportation, Washington, D.C.

Lueker, M., J. Marr, C. Ellis, V. Winsted, and S.R. Akula, 2010. *Bridge Scour Monitoring Technologies: Development of Evaluation and Selection Protocols for Application on River Bridges in Minnesota*, Report 2010-14, Minnesota Department of Transportation, Research Service Section, St. Paul, MN.

Richardson, E.V. and S.R. Davis, 2001. *Evaluating Scour at Bridges. Hydraulic Engineering Circular 18,* Fourth Edition, FHWA NHI 01-001, Federal Highway Administration, U.S. Department of Transportation, Washington, D.C

Schall, J.D., G.R. Price, G.A. Fisher, P.F. Lagasse, and E.V. Richardson, 1997a. *Sonar Scour Monitor – Installation, Operation and Fabrication Manual.* NCHRP Report 397A, Transportation Research Board, National Research Council, National Academy Press, Washington, D.C.

Schall, J.D., G.R. Price, G.A. Fisher, P.F. Lagasse, and E.V. Richardson, 1997b. *Magnetic Sliding Collar Scour Monitor – Installation, Operation and Fabrication Manual.* NCHRP Report 397B, Transportation Research Board, National Research Council, National Academy Press, Washington, D.C.

Scour Monitoring Development for Two Bridges in Texas

C. Yao[1], C. Darby[1], S. Hurlebaus[1], G. R. Price[2], H. Sharma[1], B. E. Hunt[3], O.-Y. Yu[1], K.-A. Chang[1], J.-L. Briaud[1]

[1]Zachry Department of Civil Engineering, Texas A&M University, *College Station, Texas 77843-3136, USA, Corresponding Email:* congpu.yao@gmail.com, jbriaud@civil.tamu.edu
[2]ETI, 1317 Webster Ave., Ft. Collins CO 80524
[3]STV, Incorporated, 225 Park Ave. S, New York NY 10003-1604

ABSTRACT

Bridge scour monitoring using fixed instrumentation is a good way for the owner to be warned of imminent failure and to take appropriate action before exposing the public to undue risk. This paper demonstrates two cases of bridge scour monitoring systems developed for two bridges in Texas. The lessons learned from the two systems lead the authors to the conclusion that Tethered Buried Switches for early warning and tilt sensors for warning system should be preferred. Acceleration and frequency-based behavior tracked by motion sensors show promise but could only be demonstrated in laboratory experiments, with insufficient field data.

INTRODUCTION

According to a recent study (Hunt, 2009), 58% of bridge failures result from scour, making scour monitoring a significant issue in civil engineering. Scour monitoring using fixed instrumentation is an effective method to predict the imminent failure of a bridge. The focus of this paper is to show some development in scour monitoring based on instruments, including motion sensor, tilt sensor, float-out device, water stage sensor, sonar sensor, and Tethered Buried Switch (TBS) instrument installed on two bridges in Texas.

DEVICES FOR SCOUR MONITORING

Motion sensor

The motion sensor measures the acceleration response of the bridge in three directions. In our project, it recorded the acceleration in three directions at rates of 80 Hz (field experiment) and 124 Hz (laboratory experiment).

The Japan Railway Technical Research Institute (RTRI) published a study in 2008 (Shinoda et al. 2008), which provides a new method to evaluate the stiffness of a railway bridge column called the Impact Vibration Method. The authors showed that the natural frequency of the column decreases when the stiffness of the bridge column and its foundation decrease. Thus the integrity of the column could be judged by comparing the natural frequency measured when it is known that the foundation is in good order with the natural frequency during a big flood. Inspired by this idea, we are considering using a motion sensor to monitor scour sensitive bridge columns.

Other Japanese researchers (Suzuki et al. 2007) conducted research on the health monitoring of railway bridge piers, and found that the gradient of linear regression line between vertical and transverse acceleration response changed due to the loss of sediment support around the bridge foundation. Therefore this technique is also tried in this paper by using the ratio of the Root Mean Square (RMS) of the acceleration in two directions.

TBS

The TBS (Figure 1) is a float-out device which is hardwired to the data acquisition system. It was invented during this project by ETI Instrument Systems, Inc. The TBS consists of a hollow aluminum rod containing an electrical switch which triggers when the rod is horizontal or near horizontal. The wire has advantages and disadvantages, as it might be cut by debris, but can allow the user to address the sensor and provide power. Regular float-out devices are wireless but have a finite lifetime due to the battery. The aluminum rod of the TBS is rotated to horizontal by hydraulic drag rather than buoyancy. In the horizontal direction the sensor gives a warning signal.

Other instruments

Other instruments used in our project include tilt sensor, float-out device, water stage sensor, and sonar sensor. The tilt sensor measures the tilt of the structural member to which it is attached. It is easy to install, but it likely gives a warning after the TBS and the float-out devices have floated out. The float-out device (Figure 2) floats out when the scour hole reaches the depth where the float-out device is located; when it floats out it gives a signal indicating that this scour depth has been reached. It is not easy to install for a real bridge. To bury the float-out device near the bridge pier, a hole needs to be drilled through the deck into the soil to the required depth. The water stage sensor (Figure 3) is fixed to the bridge deck and measures the distance from the instrument to the water surface. The water stage sensor can also be designed to present the water surface elevation above the mean sea level given the elevation of the bridge deck where the water stage sensor is located. The sonar sensor measures the distance between the location of the head of the sensor and the soil surface it is aimed at. It only gives reliable readings when it is within the proper working range.

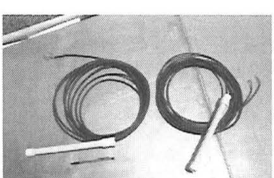

Figure 1. TBS

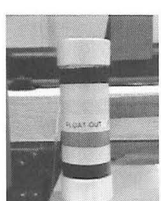

Figure 2. Float-out device

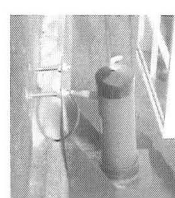

Figure 3. Water stage sensor

LABORATORY EXPERIMENT

In the laboratory experiment, the concrete column, 0.45 m in diameter and 4 m long, was embedded to a depth of 0.3 m in the sand, then two prefabricated concrete decks each 0.53 m wide, 2.03 m long, and 0.1 m thick were placed end-to-end on top of the column to simulate a bridge with a shallow spread footing foundation in the 2D flume at Texas A&M University. Motion sensor, tilt sensor, water stage sensor, sonar sensor and float-out device were used in the experiment. Figure 4 shows the illustration of the experiment setup.

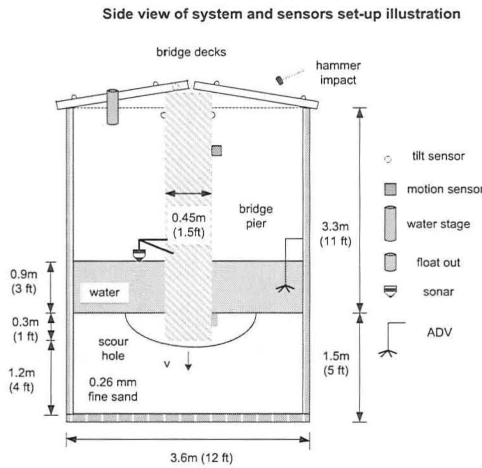

Figure 4. Experiment set-up illustration

The experiment lasted 6 hours and 45 minutes. First, the deck was struck with a 4.4 N rubber hammer. Then water was filled up to 0.9 m high in the flume, and a set of impact tests was implemented with a water velocity of 0.15 m/s, 0.3 m/s, and 0.45 m/s. It took almost 20 minutes for the test under each flowing velocity. At 0.45 m/s (3.6 hours) the scour hole started to develop. When the water velocity reached 0.6 m/s (4.5 hours), the scour hole reached the foundation level, the foundation started to be undermined, the column began to settle, and the tilt sensor indicated a change in deck inclination.

Figure 5 shows the results of the data analysis in the time domain. To study the signal in the frequency domain in detail, the acceleration trace was broken into small time intervals based on the test procedure. Figure 6 shows the relationship between the first observed frequency of the system, the ratio of RMS values of the acceleration in two directions and the tilt angle in two directions. The figure indicates that the tilt sensor reported movement at 4.5 hours after the start when the scour hole became deep enough and the column started to settle. By comparison, the frequency vs. time plots gives earlier detection (3.5 hours after the start). The ratio of RMS values in flow direction and vertical direction changes dramatically at 4.5 hours, which is consistent with the tilt sensor readings.

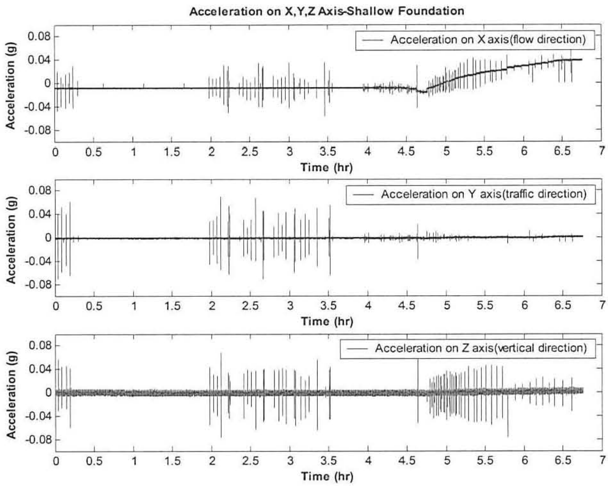

Figure 5. Acceleration in X,Y,Z axis

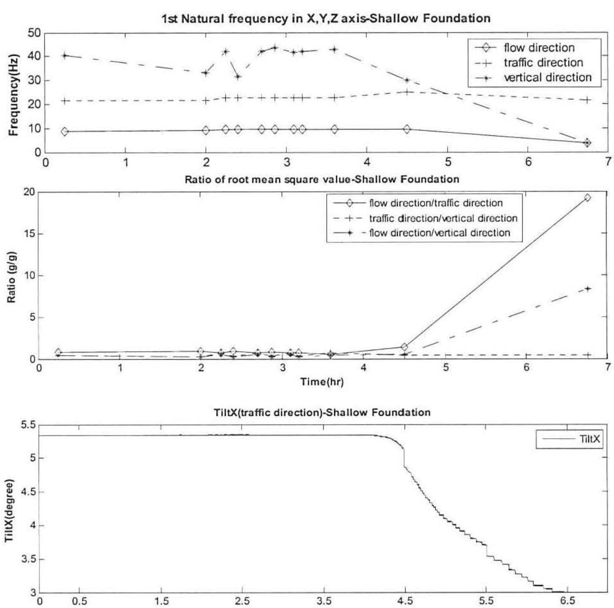

Figure 6. Comparison of frequency analysis, RMS analysis and tilt sensor reading

This experiment shows that the RMS ratio method, the FFT analysis method and the tilt sensor data give comparable results. The scour hole creates a lower stiffness of the foundation which results in a decrease in natural frequency of the column. The ratio of two RMS values of the acceleration also changes when the bridge experiences scour. Both methods can theoretically be used as warning of bridge failure due to scour.

US59 BRIDGE OVER GUADALUPE RIVER

Project background

The Southbound bridge of US Highway 59 over the Guadalupe River, south of Victoria, Texas was chosen to be monitored because the Guadalupe River is both meander-prone and flood-prone, and a drilled shaft (Figure 7) on the north end of the bridge was exposed by a major flood in 1998. The main bridge is 111 m long with three spans. It includes two river piers constructed as web-walls on foundations made of H-piles to a depth of approximately 9 m below the pile cap which is about 1 m below the river bed. The soil varies significantly, with layers of all gradations from gravel to clay, tending toward silt and sand.

Instrumentation

The instruments include a wired and a wireless motion sensor on each cap beam of the piers in the river (SB1 and SB2 in Figure 8). They are located below the deck and glued to the cap beam. One tilt sensor was bolted to the side of the bridge rail to measure the tilt angle of the deck near SB2. One water stage sensor was fixed to the side of the bridge deck near the tilt sensor to measure the water elevation. Two float-out devices were placed at a depth of 0.6 m and 1.2 m below the pile cap respectively; they were installed at the bottom of a boring near one pile cap (SB2 on Figure 8). Two TBS instruments were placed 1.5 m and 4.5 m respectively below the ground surface near the south abutment; they were installed at the bottom of a boring near the abutment. A datalogger was secured on top of the capping beam of SB2 to collect data every twenty minutes and transmit the data by cellular modem to a remote server at Texas A&M University.

Figure 7. Exposed drill shaft

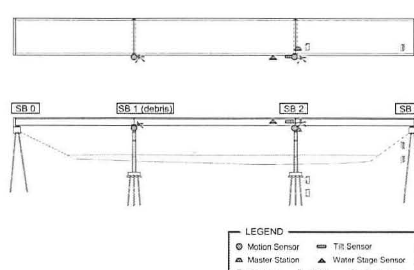

Figure 8. Schematics of instrument placement

Data analysis

Figure 9 shows the tilt sensor reading from May 28, 2009 to Feb 19, 2010. The tilt sensor indicates that very little tilt occurred on this bridge during that period. Both TBS instruments gave a constant value of 1 indicating that they remained buried. Both float-out devices gave a constant value of 0 which means that the devices were working properly and had not floated out. The water stage sensor is measuring the water surface elevation above the mean sea level (Figure 10). We also used the water gage reading from USGS gage 08176500 to check our sensor. The data for that gage can be found on the web site listed in the references. This gage is located approximately 12 km upstream of the bridge. The comparison is shown in Figure 11 and indicates a good comparison when the stage sensor was working properly.

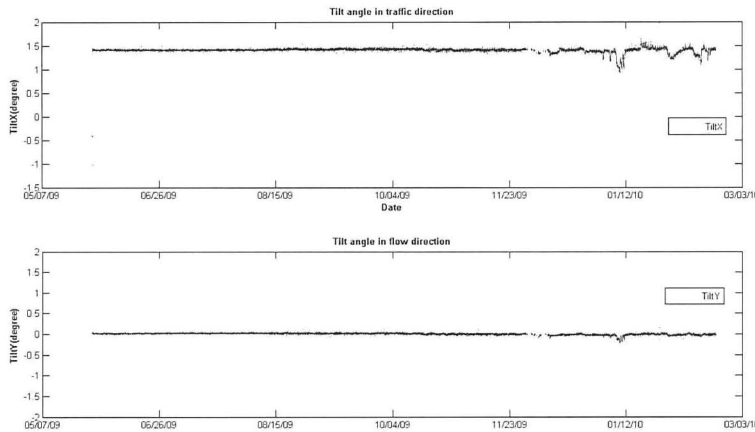

Figure 9. Tilt sensor reading from May 28, 2009 to Feb 19, 2010

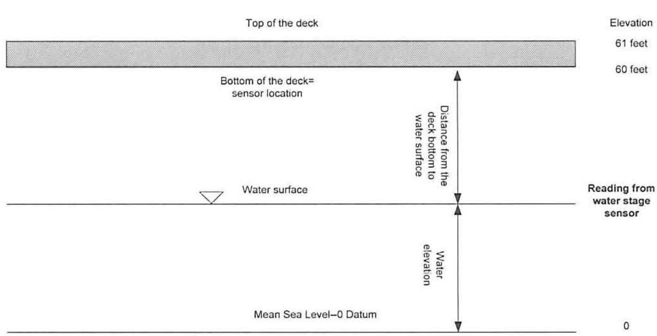

Figure 10. Description of measurement from water stage sensor

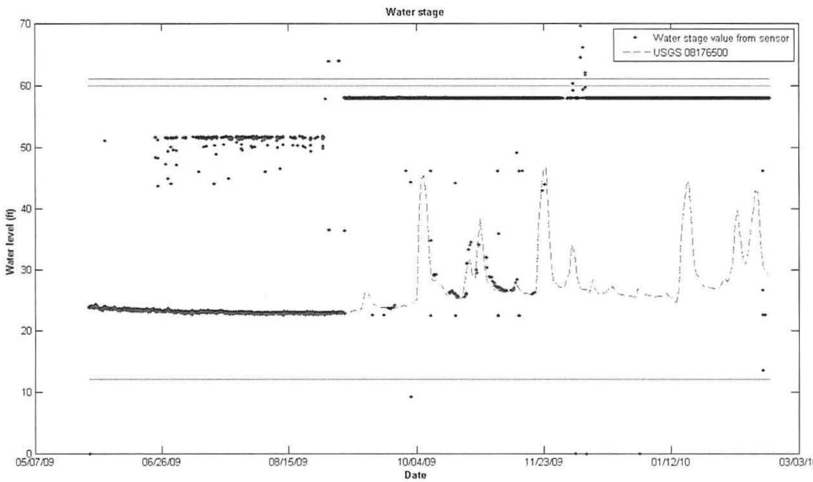

Figure 11. Water stage sensor reading from May 28, 2009 to Feb 19, 2010

A set of 148 groups of acceleration data obtained from the wireless motion sensor on US59 Bridge from June 2 @ 10:00 am to June 8, @ 13:00 pm were analyzed using the RMS method (Figure 12). As can be seen, a reasonable linear regression exists between each couple of values indicating that the ratio of the RMS values was constant during that week.

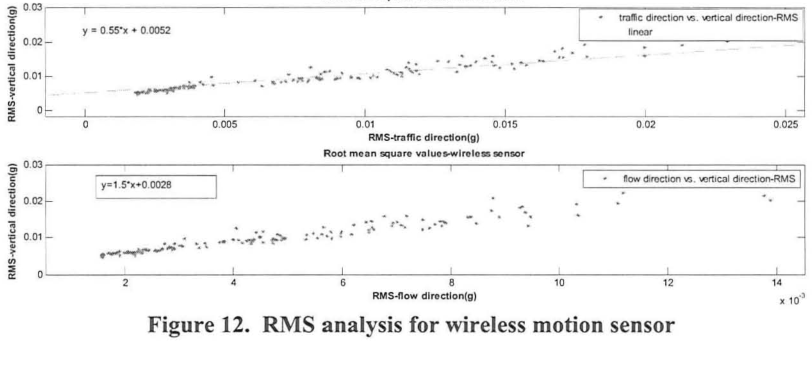

Figure 12. RMS analysis for wireless motion sensor

Discussion

The system was installed on US59 over Guadalupe River on May 28, 2009. We lost connection on the motion sensors from June 8, 2009 to October 15, 2009 because of problem with the phone company. Further problems occurred when it was realized that the solar power units were under-powered. Because of their high sampling rate, motion sensors drew more power than any other sensor, and gave difficult-to-interpret data. The acceleration response to vehicle excitation could be seen clearly but once transformed in the frequency domain, the data was very noisy and one could not distinguish different mode shapes.

While the frequency domain analysis for these motion sensors did not give a clear natural frequency for the bridge, the ratio of the acceleration RMS values from the motion sensors is a promising, simple quantity to use as a warning indicator.

In summary, the tilt sensor, the flout-out devices, the TBS, and the master station worked well while the motion sensors and the water stage did not.

SH80 BRIDGE AT SAN ANTONIO RIVER

Project background

The bridge on State Highway 80 (Figure 13) at San Antonio River, near Karnes City, was selected for implementation. It was equipped with one wireless motion sensor, one hardwired motion sensor, and two TBS instruments for scour monitoring. The data was relayed by cellular modem to Texas A&M University for data reduction.

Instrumentation

Two motion sensors were glued on the top of the center pier and the pier on the bank of the main channel respectively (Figure 13 and 14). TBS-1 and TBS2 were placed in a hand-augered borehole near the pier on the bank of the main channel. TBS1was buried 2.4 m below the ground surface and exactly 12.3 m below the top of the deck. TBS 2 was buried 1.5 m below the ground surface and exactly 11.4 m below the top of the deck. Figure 14 shows the location of the instruments for the SH80 bridge over San Antonio River.

Figure 13. SH80 Bridge

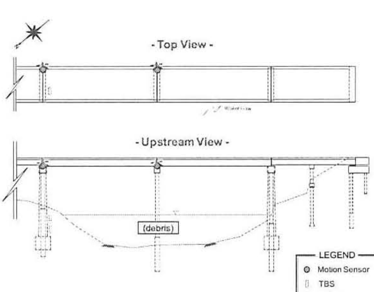

Figure 14. Schematics of instrument placement

Data analysis

Figure 15 shows that the two TBS instruments gave a value of 1 which means that the sensors were working properly and had not scoured out. The gap in the two plots corresponds to the period when the power went down. The motion sensors on this bridge did not give useful data except in December 2009.

Discussion

The monitoring system was installed on SH80 at San Antonio River on Oct 16, 2009. The hardwired sensor gave clean data in December, 2009. The wireless sensor gave clean data on Oct 20, 2009. The rest of the time the data was unsatisfactory. The motion sensors were therefore removed and replaced with tilt sensors on March 11, 2010. The TBS sensors gave clean data except for the period where there was no power.

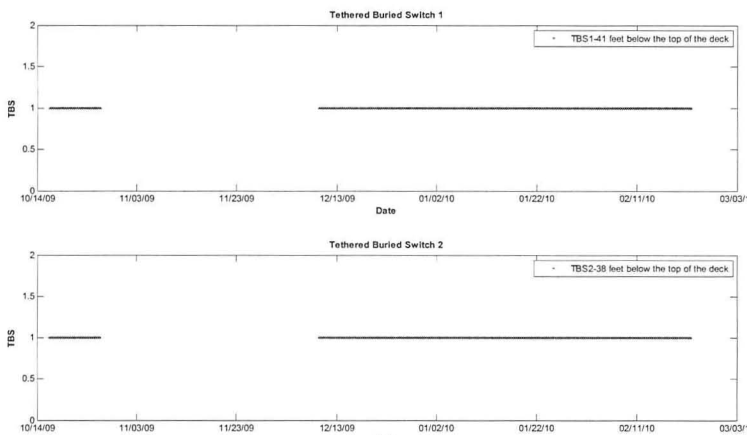

Figure 15. TBS equipment reading from Oct 16, 2009 to Feb 21, 2010

CONCLUSIONS AND SUGGESTIONS

With respect to the motion sensors, the frequency domain analysis and the acceleration ratio approach require a lot of data to be collected and stored. Therefore motion sensors require a lot of power to acquire and transmit the data in the field. The two approaches (frequency and acceleration ratio) worked well for the "model bridge" in the laboratory experiment because the structure and its vibration were simple. The response to vibrations of full scale bridges is much more complex, requires controlled and large excitation for useful data to be collected. The frequency content of the response is complex and the acceleration ratios are not consistent. So motion sensors are a good idea for bridge scour monitoring but require much more work.

Tilt sensors are reliable, simple, and relative low cost instruments. They are recommended as integrating behavior sensors which work when failure approaches. They can be helpful for other than scour.

Tethered Buried Switches are new and likely helpful, but relatively costly to install and cover only one location chosen by the engineer. They are recommended for early warning but in combination with tilt sensors. In comparison, float-out devices are likely helpful but not addressable and have limited battery life. They are recommended for short term warning systems.

ACKNOWLEDGEMENT

This project is sponsored by the Texas Department of Transportation. Marcus Galvan, John Delphia and Mark McClelland at TxDOT have been particularly helpful. We are also indebted to John Reed at Texas A&M University for his help during the laboratory experiments. Thanks very much for the tremendous help from Jason Kurten, Deeyvid Saez and Stacey Tucker during the repair of the two bridge monitoring systems.

REFERENCES

Briaud, J.-L., Yao, C., Darby, C., Sharma, S., Hurlebaus, S., Price, G.R., Chang, K.A., Hunt, B.E., Yu, O.-Y. Motion Sensors for Scour Monitoring: Laboratory Experiments and Numerical Simulations. The *Transportation Research Board (TRB) 89th Annual Meeting*. Washington, D.C. January 10-14, 2010.

Darby, C., Yao, C., Hurlebaus, S., Price, J., Hunt, B.E., Yu, O.Y., Chang, K.-A., Briaud. J.L. Motion Sensors for Bridge Scour Monitoring: Preliminary Laboratory and Field Experience. *Texas Section-ASCE fall 2009 meeting*. The Woodlands, Texas. October 28-31, 2009.

Hunt, B. E. (2009) "Monitoring of Scour Critical Bridges." *NCHRP Synthesis of Highway Practice 396,* Transportation Research Board, Washington, D.C.

Suzuki, O., Abe, M., Shimamura, M., Matsunuma, M. A Health Monitoring System for Railway Bridge Piers. *The 3rd International Conference on Structural Health Monitoring of Intelligent Infrastructure*, Vancouver, British Columbia, Canada, November 13-16, 2007.

Shinoda, M, Haya, H., Murata, S. (2008) "Nondestructive Evaluation of Railway Bridge Substructures by Percussion Test." *Fourth International Conference on Scour and Erosion (CD-ROM)*, Tokyo, Japan.

Yao, C., Darby, C., Yu, O.-Y., Hurlebaus, S., Chang, K.A., Price, J., Hunt, B., Briaud. J.-L. Motion Sensors for Scour Monitoring: Laboratory Experiment with a Shallow Foundation. Proceedings of *GeoFlorida 2010*, West Palm Beach, Florida. February 20-24, 2010. ASCE

http://waterdata.usgs.gov/tx/nwis/uv?site_no=08176500&format=gif&period=31

Monitoring Hydraulic Conditions and Scour at I-90 Bridges on Blackfoot River Following Removal of Milltown Dam near Bonner, Montana, 2009

By Stephen R. Holnbeck[1] and Peter M. McCarthy[2]

[1]U.S. Geological Survey, 3162 Bozeman Avenue, Helena, MT 59601; PH (406) 457-5929; email: holnbeck@usgs.gov
[2] U.S. Geological Survey, 3162 Bozeman Avenue, Helena, MT 59601; PH (406) 457-5900; email: pmccarth@usgs.gov

ABSTRACT

Following the 2008 removal of Milltown Dam on the Clark Fork, the U.S. Geological Survey, in cooperation with the U.S. Environmental Protection Agency, began a multi-year monitoring effort to evaluate hydraulic and scour conditions at the I-90 bridges located 0.44 kilometers upstream on the Blackfoot River. The profile of water-surface elevation surveyed at the 1.5-year recurrence interval peak flow (bankull discharge) indicated substantial bridge contraction and complex hydraulics. Maximum measured pier scour of 1.2 meters was likely limited by argillite bedrock underlying the gravel and cobble streambed. Velocities measured within the contracted bridge opening at bankfull discharge exceeded the 1.83 meters per second considered favorable for bull trout (*Salvelinus confluentus*) passage, except perhaps at the very bottom and along the edges of the channel. Bathymetric surveys indicated substantial changes in channel geometry within the study area since the removal of the dam, which also is evident in shifts of stage-discharge rating curves.

INTRODUCTION

The 2008 removal of Milltown Dam on the Clark Fork, near Bonner, Montana, was predicted to affect pier and abutment foundations of nearby bridges. The substantial contraction of streamflow at the bridges was expected to exert hydraulic forces on these structures not experienced when the bridges were in the backwater of Milltown Reservoir. The bridges are located near the confluence with the Clark Fork and are part of U.S. Interstate 90 (I-90), a major transportation corridor through Montana. Countermeasures used to mitigate predicted scour and erosion included substantial modification to the piers and abutments of the I-90 bridges that cross the Blackfoot River 0.44 kilometers (km) upstream from the dam near the confluence with the Clark Fork. Dam removal enables bull trout (*Salvelinus confluentus*), listed as threatened under the Endangered Species Act, to reach critical habitat in the headwaters of the Blackfoot River. However, fish must first pass through the contracted I-90 bridge opening during spring runoff when high velocities might inhibit fish passage.

The U.S. Geological Survey (USGS), in cooperation with the U.S. Environmental Protection Agency (USEPA), began monitoring hydraulic and scour conditions at the I-90 bridges prior to the spring 2009 runoff season, following dam removal. The purposes of the multi-year monitoring are to measure effects of streamflow conditions on the I-90 bridge pier and abutment structures and nearby stream channel morphology, obtain hydraulic and scour data to calibrate and verify hydraulic models, and collect stream-velocity data that would be used to evaluate whether bull trout can swim upstream through the contracted bridge opening during spring runoff.

STUDY AREA

The Blackfoot River, a snowmelt-dominated coarse-bed stream in western Montana, has a drainage area of about 5,931 square kilometers (km^2) upstream from two highway bridges that span the river near Bonner (fig. 1). About 0.44 km downstream is the former site of Milltown Dam and reservoir, a low-head hydroelectric facility on the Clark Fork, where sediments enriched in trace elements from more than 100 years of historical mining had been deposited since the construction of the dam in 1907. The removal of Milltown Dam was completed in 2008 as part of the USEPA Superfund remedial activities.

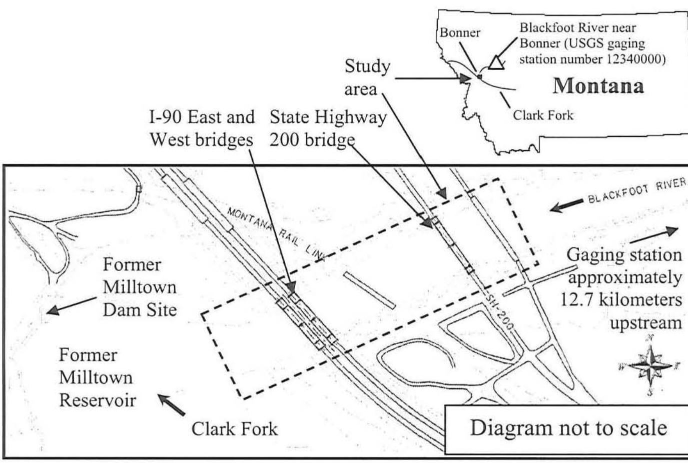

Figure 1: Diagram showing location of the study area before dam removal (P.D. Smith, CH2MHILL, written commun., 2010).

The I-90 bridges consist of two identical two-lane structures that convey eastbound (I-90 East) and westbound (I-90 West) traffic. The continuous steel girder bridges were completed in 1964 and have a total length of about 104.5 meters (m) and a maximum clear span of about 38.3 m. The support for the main span of each bridge is a single cylindrical pier 3.05 m in diameter located at midspan within the main channel of the Blackfoot River. The end supports for the main span of each bridge are two bridge pilings, or bents, located about one-halfway up the embankments out of the river. The pilings also support two shorter approach spans. The original foundation for the center pier is a spread footing excavated into riverbed alluvium.

The footing seal is likely to be in contact with argillite bedrock having a rough and uneven surface (CH2MHill, 2006a). Boring logs at stations locating the I-90 East and I-90 West piers indicate a gravel layer 0.12 m thick at the concrete seal and argillite interface.

The original foundation design for the center pier was based on the assumption that backwater conditions created by Milltown Reservoir would persist throughout the service life of the bridges; thus, velocities would always be low and scour would not be a problem. Spread footings for the center piers were, therefore, considered a valid design. With the dam removed, however, seasonal flood velocities in the Blackfoot River through the I-90 bridge openings were predicted to cause pier scour problems (CH2MHill, 2006b).

Countermeasures chosen to mitigate predicted pier scour included underpinning the spread footings with multiple drilled shafts that extend into the argillite. The size of the footings and seals also were increased by encasing the drilled shafts in reinforced concrete. Micro-pile walls and jet-grout columns were constructed just down slope from the bridge pilings supporting the approach spans to mitigate slope-stability concerns. Rock riprap and interlocking concrete armor units (A-Jacks) were placed on the bank up to the predicted 500-year water-surface elevation. A-jacks were placed at a 2:1 slope to improve slope stability and provide scour protection. These countermeasures result in a substantial bridge contraction that increases the severity of local hydraulic conditions relative to natural conditions. The ratio of uncontracted- to contracted-flow width (contraction ratio) was measured to be about 2.0 at the 1.5-year recurrence interval flood.

METHODS

Monitoring activities at the site included using fixed instrumentation to continuously measure pier scour and stream stage, conducting bathymetric and topographic surveys, and conducting periodic site visits to measure flow depths and velocities. Acoustic transducers were fixed to each pier to measure real-time pier scour and consisted of four 8-degree beam angle, 235-kilohertz transducers. A non-submersible pressure transducer, attached to an orifice line located on the downstream side of the I-90 East pier, was installed to measure and record stream stage. A pulse-radar unit was installed to measure stage at the State Highway 200 bridge (SH 200) located about 260 m upstream. Transducers and stage-recording devices were linked to a data-collection platform (DCP) and Geostationary Operational Environmental Satellite (GOES) transmitter to log and transmit data in real-time. Streamflow was recorded at the USGS gaging station Blackfoot River near Bonner, Mont. (12340000), located about 12.7 km upstream. No large tributaries flow into the Blackfoot River between the gage near Bonner and the study area.

Streambed bathymetry and topographic surveys were conducted before and after the 2009 runoff season in the study area. A land-based robotic total station was used to survey the river reach in the study area when the river could be waded (fig. 1).

The robotic total station was paired with a boat-based survey-grade echo sounder to survey the bathymetry when flow conditions prohibited wading. Survey data were used to identify locations where the channel scoured or filled and to provide data for calibration and verification of hydraulic models constructed by other agencies.

In addition to data from permanently installed instruments and survey data, other hydraulic data were measured during site visits including water depth, water-surface elevations for constructing water-surface profiles, and flow velocity. Hydraulic data associated with the 1.5-year recurrence interval peak streamflow of 198 meters per second (m^3/s) were collected because this streamflow approximates bankfull discharge and is the streamflow for which hydraulic data were sought for assessing the likelihood of bull trout passage. Flow depth and velocity were measured using an acoustic Doppler current profiler (ADCP) at cross sections located upstream and within the contracted I-90 bridge opening. Depth and velocity and depth data were obtained both laterally across the section and in the vertical profile. Velocity was measured at an uncontracted approach section, a partially contracted section, and a fully contracted section. The ADCP was mounted on a tethered boat and was held stationary at positions along selected cross sections. Turbulence, air entrainment, and standing waves prevented high-flow measurements downstream from the piers where the stream widens.

MONITORING RESULTS AND DISCUSSION

At the end of the first year (2009) of study, a preliminary analysis of the data was conducted. It is apparent from the analysis that the removal of Milltown Dam has altered the hydraulic conditions in the study area. These altered conditions have changed the effect of the I-90 bridges on the channel morphology of the Blackfoot River in the study area. Because results reflect a single year of monitoring, more comprehensive conclusions can not be made until multiple years of data are obtained.

Flow impingement and obstruction of flow on the upstream face of the 6.7-m wide I-90 West bridge pier footing causes complex hydraulic conditions during high flows. The obstruction splits the flow to either side of the footing and results in two different water-surface profiles to the right and left of the piers of each bridge (fig. 2). Other hydraulic conditions observed during 2009 runoff at the piers included turbulent flow on the backside of the footings, flow separation zones that propagated downstream from footings, vortices on the sides of the footings, rollers, and standing waves in the expanding reach downstream from the bridge opening. Water-surface elevations surveyed on June 1 indicated a substantial drop of 1.36 m (fig. 2) through the bridge when the flow equaled 277 m^3/s, slightly in excess of the 2-year recurrence interval. Water-surface elevations surveyed on March 31 indicate that the I-90 bridges have little impact on the flow profile for low-flow conditions.

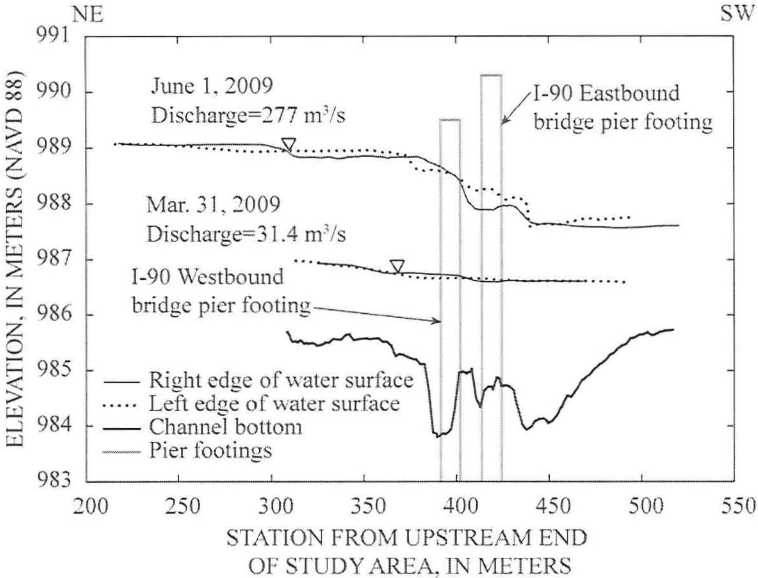

Figure 2: Water-surface profiles, channel bottom, and pier footing locations for the I-90 bridges through the study area.

Four acoustic transducers were fixed to the bridge piers in March 2009 to continuously measure scour and fill. Only one transducer (T1) operated successfully because turbulence and air entrainment in the water column hindered the performance of the other transducers. Maximum total scour equal to 1.2 m was measured on the left upstream side of the I-90 West pier, and reflected the net effects of both pier scour and contraction scour components. Although scour depth typically increases as flow increases, scour response at the site was more complex and lagged behind the initial short-duration peak flow recorded on May 20 (fig. 3). Instead of scouring on May 20, scour began on the second rising limb of the runoff hydrograph recorded on May 24 and reached maximum depth on May 25 for a peak flow slightly less than the May 20 peak of 272 m^3/s. The lag in scour may have been caused by weakening of the armor layer during the first peak, followed by rapid scour on the second rise of the hydrograph. Another possibility was that the rate of transport into the scour hole on the first peak was similar to the rate of transport out of the scour hole under live-bed scour conditions, with only minor net scour taking place.

The streambed elevation measured by transducer T1 remained very near the May 25 scoured level well into November 2009, with some minor infilling. Pier scour measured on May 25 was only about 30 percent of pier scour predicted by the HEC-18 equation (Richardson and Davis, 2001) and may have been limited by scour resistant argillite bedrock underlying the gravel and cobble streambed. Pier and contraction scour extended downstream (fig. 2) to about station 500, near the confluence with the Clark Fork.

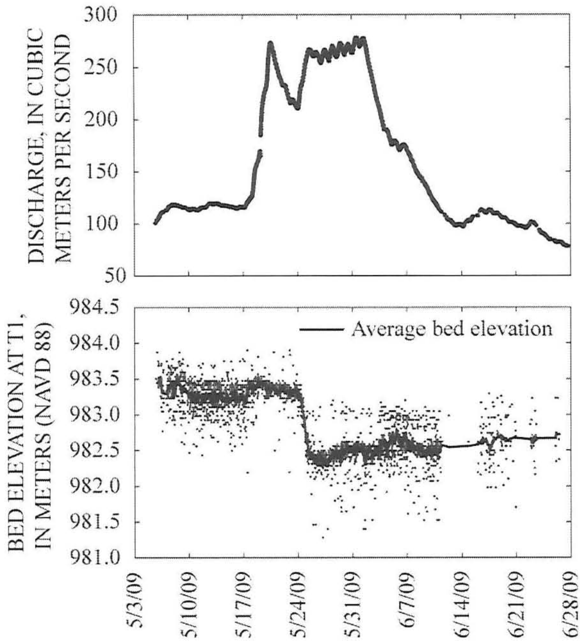

Figure 3: Blackfoot River hydrograph and bed elevation at transducer T1 located on left side of the upstream I-90 bridge pier.

Streambed bathymetry and topographic surveys of bridge abutments and embankments were conducted before and after 2009 runoff. The survey data were used to generate cross sections and water-surface profiles and to develop the computational mesh for two-dimensional hydraulic modeling. A cross section in the contracted reach (fig. 4) between the I-90 East and West piers indicates maximum residual scour in the left channel of about 1.2 m and maximum residual scour in the right channel of about 1.0 m. Scour is least in midchannel because of the sheltering effect provided by the I-90 pier footings. Erosion of the left and right abutment toe and settlement of the right A-Jack embankment also is evident and reflects damage that required major repair in 2010. Examination of other cross sections indicated that most of the study reach experienced net scour similar to that shown in figure 4.

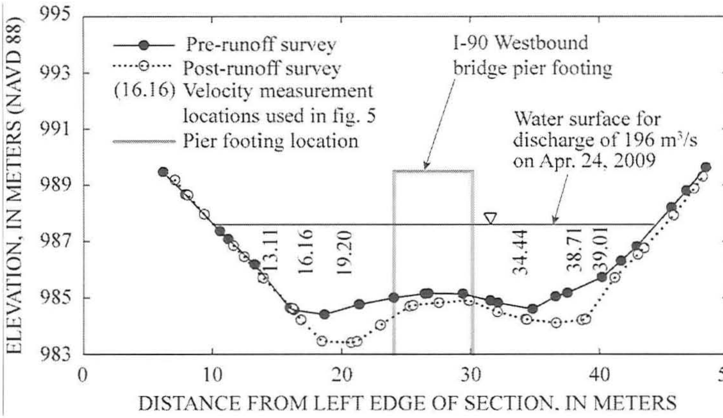

Figure 4: Cross-section geometry looking downstream showing the locations of the upstream pier and measured velocity profiles for cross section located between the I-90 piers.

Velocity-profile measurements provided data for the evaluation of the likelihood of bull trout passage through the study area. Channel velocities less than 1.83 m/s are considered favorable for bull trout passage (G. D. Beattie, CH2MHILL, written commun., 2009). In the study area, fish passage is most limited where flow is split into two channels by the pier footing for the I-90 West bridge and velocities are greatest. Velocity-profile data were collected at six stations along a cross section with split flow (fig. 4) by holding an ADCP stationary for up to 5 minutes at each station while velocity data were logged. This approach is based on the midsection method (Mueller and Wagner, 2009), where the measured water velocity is not biased by moving-bed conditions. Velocity-profile measurements (fig. 5) were made on April 24, 2009, when the flow (196 m^3/s) approximated bankfull discharge. Velocity could not be measured near the streambed and water surface because of limitations inherent in the ADCP technology and were estimated by curve extension (Teledyne RD Instruments, 2007). Measured flow velocities for the six stations at bankfull discharge exceed velocities deemed favorable for bull trout passage. Flow velocities favorable for bull trout passage (< 1.83 m/s) may only exist near the channel bottom or perhaps along the channel edges. Average velocities at bankfull discharge obtained for the uncontracted approach section, partially contracted section, and a fully contracted section were equal to 1.82 m/s, 2.30 m/s, and 3.46 m/s, respectively. Average velocity through the fully contracted bridge opening is, therefore, almost twice the velocity indicated in the uncontracted approach section considered typical of natural conditions.

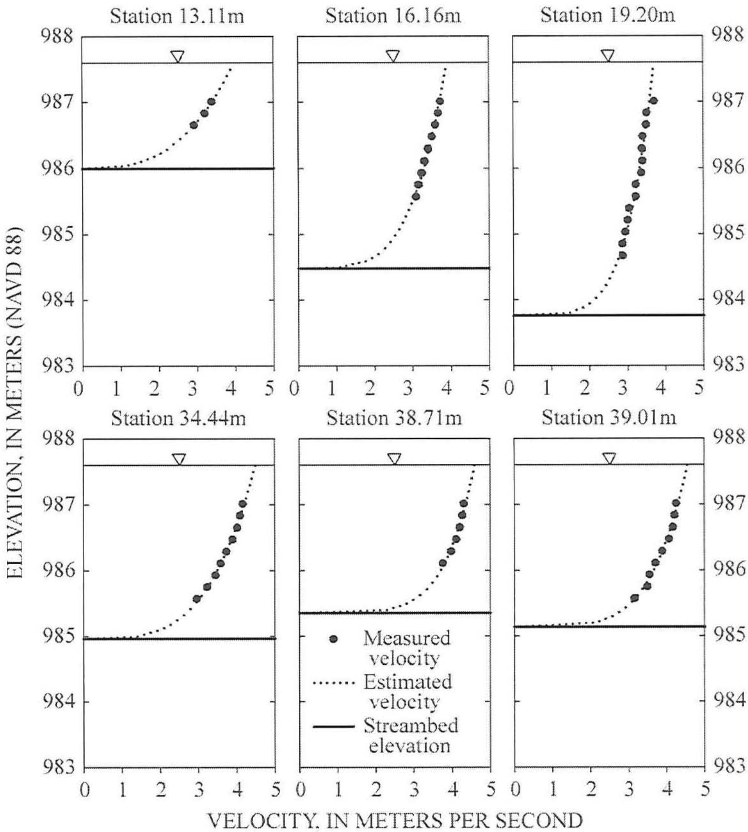

Figure 5: Velocity profiles for cross section (fig. 4) located between I-90 East and I-90 West bridge piers.

Stream stage at the I-90 and SH 200 bridges and streamflow data for the USGS gage at Blackfoot River near Bonner were used to develop stage-discharge rating curves (fig. 6) for the study area. Rating-curve shifts were computed to provide a means for assessing stream stability (Lagasse, 1991). A continued shift in one direction over the long term can indicate a stream reach is aggrading or degrading. The I-90 rating curve reflects stage-discharge conditions for a reach where flows exit the I-90 bridge contraction and the stream expands to the confluence with the Clark Fork. The I-90 rating curve had no detectable shift at higher flows but shifted to the left when flow dropped to about 100 m^3/s on the falling limb of the spring 2009 hydrograph (fig. 6). Substantial deposition of gravel and small cobbles took place at the mouth of the Blackfoot River on the falling limb of 2009 runoff and is the likely cause for the shift observed in the I-90 rating curve.

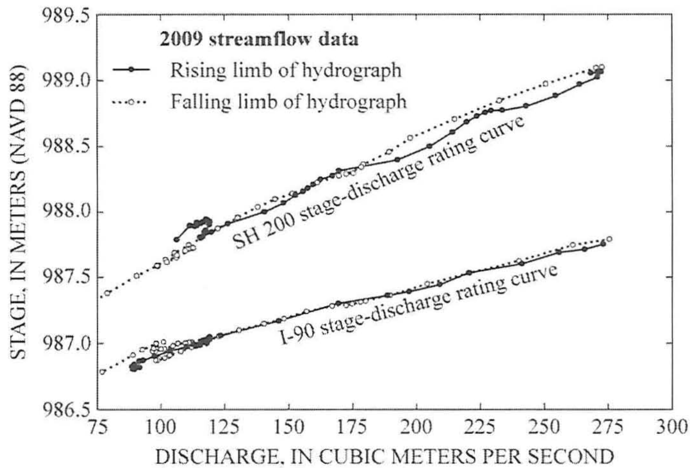

Figure 6: Blackfoot River stage-discharge rating curves used to assess stream stability at two locations in the study area.

The SH 200 rating curve reflects stage-discharge conditions for a reach located upstream from the I-90 bridges. The rating curve shifted substantially to the right on the rising limb of the hydrograph (fig. 6) when flow reached about 110 m^3/s, indicating channel scour. The SH 200 rating curve shifted slightly to the left throughout much of the falling limb of the hydrograph indicating channel infill. The net rating curve shift for the 2009 runoff hydrograph was to the right due to the substantial shift on the rising limb of the hydrograph. A net shift to the right indicates that scour predominated over the 2009 runoff period in the SH200 reach. Comparison of pre- and post-runoff cross-section data indicate that residual scour prevailed in the reach reflected by the SH200 rating curve. Multi-year monitoring of rating-curve shifts at the two sites could provide a better indication of channel stability in the study area and identify trends, if any, that are taking place.

SUMMARY

Piers and abutments of the I-90 bridges crossing the Blackfoot River near Bonner, Montana, underwent substantial modification to mitigate scour and erosion concerns resulting from the 2008 removal of Milltown Dam, located approximately 0.44 km downstream on the Clark Fork. Substantial contraction of flow at the bridges during spring runoff was expected to cause severe hydraulic conditions that might cause bridge scour and impede passage of threatened bull trout. Consequently, the USGS and USEPA began monitoring hydraulic and scour conditions at the I-90 bridges prior to the spring 2009 runoff season. The purposes of the multi-year monitoring include measuring effects of streamflow conditions on the I-90 bridge pier and abutment structures and nearby stream channel morphology, obtaining hydraulic and scour data for model calibration and verification, and collection of stream velocity data to evaluate the likelihood of bull trout passage.

Results thus far indicate that the profile of surveyed water-surface elevation at bankfull discharge dropped 1.36 m through the contracted bridge opening. Maximum total pier scour of 1.2 m was measured, but the argillite bedrock underlying a gravel and cobble streambed may have limited scour. Streamflow velocities measured at bankfull discharge exceeded the 1.83 m/s considered favorable for bull trout passage. Velocities less than 1.83 m/s may only exist very near the channel bottom or on the channel edges. Stage-discharge rating curves were developed for two locations in the study area to assess channel stability, however, multi-year monitoring at the two sites would provide a better assessment. Results were presented for a single year of monitoring, and comprehensive conclusions will require the interpretation of results obtained over multiple years.

REFERENCES

CH2MHILL, (2006a). "Geotechnical report for the Milltown Reservoir bridge mitigation project." *CH2MHILL*, Boise, ID, 75 p.

CH2MHILL, (2006b). "Milltown bridge infrastructure mitigation hydraulics report." *CH2MHILL*, Boise, ID, 29 p.

Lagasse, P.F., Schall, J.D., Johnson, F., Richardson, E.V., and Chang, F. (1991). "Stream stability at highway structures." *U.S. Depart. of Transportation Pub. FHWA-IP-90-014, Hydraulic Engrg Circ. 20*, Arlington, VA, 195 p.

Mueller, D.S., and Wagner, C.R. (2009). "Measuring discharge with acoustic Doppler current profilers from a moving bed." *U.S. Geol. Survey TM 3A-22*, Reston, VA, 72 p. (available online at http://pubs.water.usgs.gov/tm3a22).

Richardson, E.V., and Davis, S.R., (2001). "Evaluating scour at bridges." *U.S. Depart. of Transportation Pub. FHWA NHI 01-001, Hydraulic Engr Circ. 18*, Arlington, VA, 378 p.

Teledyne RD Instruments, (2007). "WinRiver II user's guide." *Teledyne RD Instruments*, Poway, CA, 162 p.

Modeling and Monitoring Scour during Bridge Replacement with Multi-dimensional Modeling and Repeated Multi-beam Surveys at the Tanana River near Tok, Alaska

J.S. Conaway[1]

[1]U.S. Geological Survey Alaska Science Center, 4210 University Drive, Anchorage, AK, 99508; PH (907) 786-7041; email: jconaway@usgs.gov

ABSTRACT

The Alaska Highway near Tok, Alaska crosses the Tanana River via a 288 m truss bridge constructed in 1944. Due to age, damage from a 2002 earthquake, and extensive pier scour, the bridge is being replaced in 2009-2010. Since it was originally constructed, the angle of approaching flow to the bridge has changed and currently approaches the right-bank pier at 45 degrees creating a large scour hole around the pier. The new bridge is being constructed 75 meters downstream of the existing bridge and a temporary construction causeway was built in 2009 upstream of the new bridge alignment. The effect of the causeway on the channel hydraulics at the existing bridge are of concern to ADOT&PF. Several potential causeway geometries and their corresponding affect on the angle of flow approaching the existing bridge pier were simulated with a multi-dimensional model. Modeled flow angles, depths, and velocities immediately upstream of the pier did not vary significantly between the modeled scenarios, but a monitoring schedule was put in place to insure the safety of the structure until the new bridge is completed. Four multi-beam surveys completed during the summer of 2009 documented the dynamic nature of the streambed. The largest scour depths were consistently at the nose and along the right-bank side of the caisson where the flow was attacking the pier. Model results and repeated high accuracy surveys allow the state to continue operation of the bridge and avoid installing scour countermeasures until construction of the new bridge is completed.

INTRODUCTION

The Alaska Highway, which is Alaska's main land arterial with Canada and the contiguous United States, crosses the Tanana River near Tok, Alaska, via a bridge that is nearly 60 years old. Age, a narrow bridge deck, damage from an earthquake, and observed streambed scour at the bridge have led to the Alaska Department of Transportation and Public Facilities' (ADOT&PF) decision to replace the structure. The new bridge is being constructed 75 m downstream of the existing structure.

The Tanana River near Tok drains an approximately 17,600 km^2 glaciated basin north of the Alaska Range. At and near the study reach, the river is extensively braided and carries a high suspended-sediment load. The riverbed is composed of silt and sand, and dune movement has been observed over a range of stages. The riverbanks are composed of unconsolidated silt and sand, with the exception of the right bank that is composed of granitic bedrock from the existing bridge to the downstream extent of the study reach. Overbank vegetation is predominately dense spruce and willow. The existing bridge is located where the river enters a natural constriction that is controlled by the bedrock along the right bank. As the river approaches the bridge on the right bank, it is directed by the bedrock at an angle to the long axis of the pier. This flow angle of attack on the pier has been observed to be approximately 40 to 45 degrees at a streamflow of 725 m^3/s. The high angle of attack on the pier and position of the bridge at the head of a natural constriction, where flow velocities and sediment transport capacity are the highest, make this structure particularly susceptible to streambed scour.

The existing bridge, ADOT&PF bridge number 505, is located at mile marker 80.5 of the Alaska Highway. It is 288 m long, 7 m wide, and was constructed in 1944. Two sloping sharp-nosed piers that are surrounded by sheet pile caissons support the bridge. The piers are 2.4 m wide and 15.8 m long. The caisson surrounding the piers is 7 m wide, 20 m long and extends above the water surface at medium flows. The new bridge is being constructed from temporary earthen and pile supported causeways (Figure 1). The causeways were constructed in September 2009 and are scheduled to be removed by April 2010 before the spring breakup. The left causeway extends approximately 30 m from the left bank and is connected to an approximately 110 m long center causeway located on a natural bar that is exposed during low flows. Cylindrical piles support two bridge decks, one connecting the two causeways and another extending from the center causeway into the channel toward the right bank.

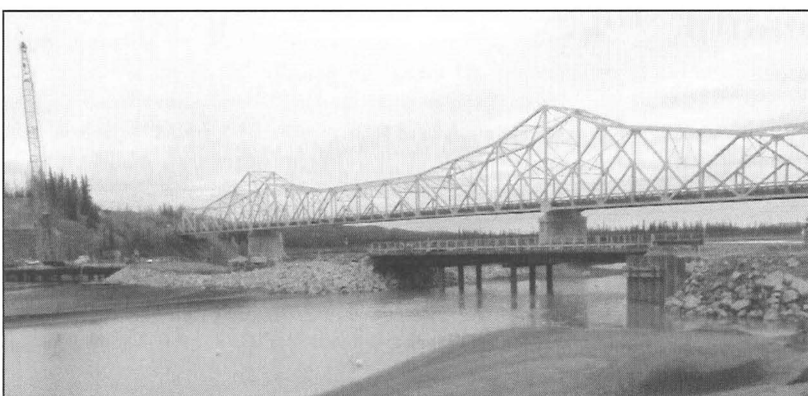

FIGURE 1: Upstream view of the two causeways and bridge 505 near Tok Alaska. Photographed on October 9, 2009 at a streamflow of 112 m^3/s.

The U.S. Geological Survey (USGS) collected continuous daily streamflow information at the bridge (gaging station No. 15472000) from 1950 to 1953 (U.S. Geological Survey, 1951-1954). The mean annual streamflow of the Tanana River near Tok Junction during that period of data collection was 197 m^3/s. During late May or early June, a period of high flow associated with snowmelt runoff begins. High flow persists typically through July and August reflecting glacial melt and periods of rainfall. High flows also result from intense rainfall in the late summer and low flows precede freeze up in late October to early November. Annual peak flows from 1950 to 1953 were 889, 889, 796, and 988 m^3/s, respectively. The slope of the river through the bridge is 0.0002 m/m. The USGS surveyed water depths and velocities in August 2002 to develop and calibrate a multi-dimensional flow model for simulating high-flow water-surface elevations and velocities (Conaway and Moran, 2004).

Annual channel cross sections have been surveyed at the bridge since 2002 and scour depths at the right bank pier have extended to the base of the caisson. The susceptibility of this pier to scour prompted an analysis using a multi-dimensional flow model to simulate the potential backwater effects of the caissons 75 m downstream of the bridge. In addition to the modeling effort a monthly channel surveying schedule was established to track channel changes around the scour-critical pier during construction. Scour monitoring was chosen instead of installing scour countermeasures for a bridge that is scheduled for replacement.

SURFACE WATER MODELING

The USGS Multi-Dimensional Surface Water Modeling System (MD_SWMS) (McDonald and others, 2005) was used to simulate the initial conditions and the potential causeway geometries to determine the effects on velocity and depth at bridge 505. MD_SWMS is a generic interface developed by the USGS for hydrodynamic models. FaSTMECH, one of the computational models within MD_SWMS (Nelson and McDonald, 1997), is a 2-dimensonal, vertically-averaged, steady state model that was selected for this study. The initial conditions scenario was created with bathymetry data collected in 2002 (Conaway and Moran, 2004) and updated with bathymetry collected in 2009 at the bridge. The model was calibrated with water-surface elevations, flow velocities, and flow directions collected at a streamflow of 725 m^3/s when the 2002 bathymetry was collected (Conaway and Moran, 2004). A second scenario was modeled with the bathymetry from the initial conditions and was modified to reflect the elevation and extents of the two causeways.

Four streamflows; 300 m^3/s, 425 m^3/s, 566 m^3/s, and 866 m^3/s (2–year recurrence interval flow) were simulated with each model. These flows represent the range of streamflows that could be expected during the life span of the project. At 300 m^3/s, the river is divided into two channels through the bridge reach and the only effect of the causeways is the constriction of flow between them along the left bank. At 425 m^3/s, the right bank portion of the channel becomes constricted by the causeway and simulated velocities are increased in that area. The effects of the channel constrictions become more pronounced at 566 m^3/s. Velocities on the downstream side of the left bank pier are reduced in the causeway simulations because more flow is diverted to the right bank portion of the channel by the center causeway. The causeways are completely overtopped at 866 m^3/s. The likelihood of this streamflow occurring during the lifespan of the causeways is extremely low because high flows have historically occurred only in July and August.

To evaluate potential impacts at the right bank pier of the existing bridge the predicted depth, velocity, and Froude number were extracted from both models along a cross section immediately upstream of the pier. The results were similar for all simulations except at the highest streamflow. The predicted depths were up to 0.4 m higher to the left and the right of the pier for the causeway scenario (Figure 2). Velocities and Froude numbers were not however significantly different. The increased depths are the result of more flow being distributed to this portion of the channel as a result of the center causeway.

The modeling results from the two scenarios do not indicate that the causeways will have an impact on conditions that cause scour at the right bank pier. Predicted flow depths were greater for the causeway scenario at the highest streamflow, but not immediately upstream of the pier, only to the left and right of the pier. Pier scour was computed for both scenarios using the CSU pier scour equation with the bed armoring coefficient (Richardson and Davis, 2001) (Table 1). The scour computations were made using the geometry of the caisson because only a small portion of the pier stem is in the water column. The angle of attack for the approaching flow, 45 degrees, was the same for both scenarios Predicted scour only increased by 0.1 m for the causeway scenario.

TABLE 1: Computed pier scour from modeled values for the initial conditions and causeway scenario.

	Initial Conditions	Causeway
Froude number	0.19	0.20
Angle of Attack	45	45
Pier Shape	Round	Round
Pier Width (m)	7.01	7.01
Pier Length (m)	19.81	19.81
Depth (m)	*6.07*	6.08
Velocity (m/s)	0.98	1.01
D50 (mm)	9.10	9.10
D95 (mm)	41	41
Bed Armoring (k4)	0.4	0.4
Computed Pier Scour	**5.49**	**5.61**

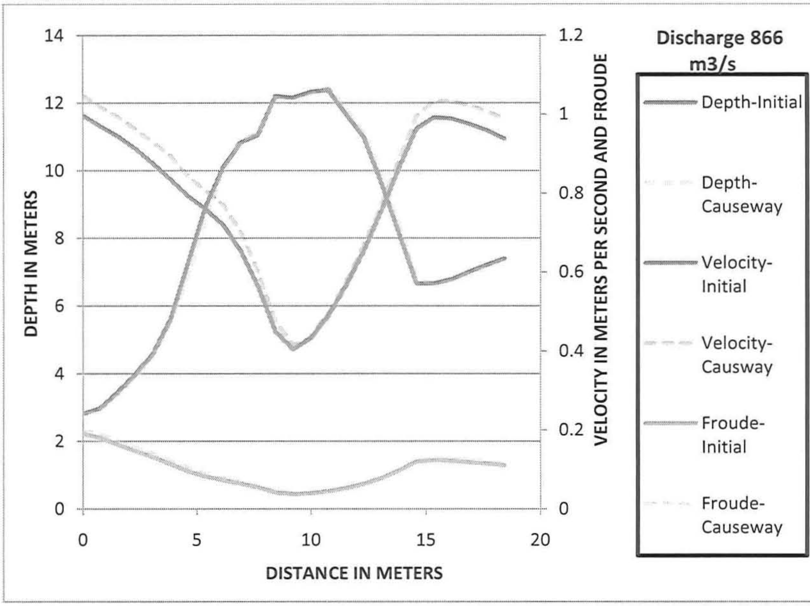

Figure 2: Model results from both the initial and causeway scenarios for a cross section immediately upstream of the right-bank pier.

STREAMBED SCOUR MONITORING

An analysis of streambed scour potential by Heinrichs and others (2001) estimated 8.5 m of pier scour for the 100-year recurrence interval streamflow. Cross sections along the upstream side of the bridge and profiles along the right bank pier have been surveyed annually since 2002 (Figure 3). Several of these surveys indicated that the bed elevations at the right bank pier were below the bottom of the caisson. The seasonality of streamflow and sediment load result in a seasonal pattern of streambed scour and fill where bed elevations rise during fall and winter and then decrease during the spring and summer. This pattern was described by Conaway (2006, 2007) in an analysis of continuous streambed elevation datasets from other glacially-fed rivers in Alaska.

Streambed elevations around the right-bank caisson were mapped four times in 2009 over a range of streamflows (6/2/09, 240 m^3/s; 7/1/09, 362 m^3/s; 8/5/09, 736 m^3/s; 10/7/09, 112 m^3/s) to monitor bed elevations. Bathymetry data were collected using a 1200 kHz acoustic Doppler current profiler (ADCP) interfaced with a differentially

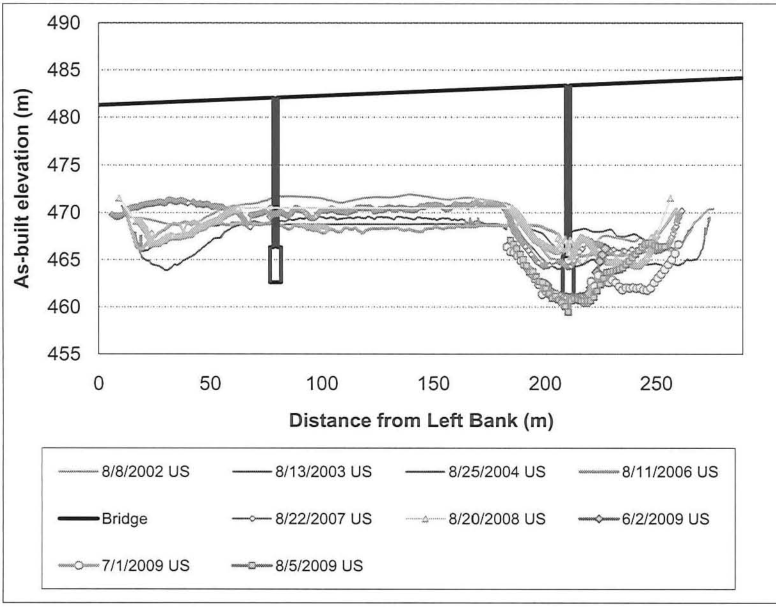

Figure 3: Surveyed cross sections along the upstream side of bridge 505.

corrected GPS. The ADCP uses four transducers oriented 20 degrees from vertical to emit acoustic pulses that are scattered and reflected from particles in the water column back to the transducers. Frequency differences between the transmitted and received pulse are combined with boat speed information to resolve a 3-dimensional water velocity. The ADCP uses reflections from the stream bottom to determine boat speed and flow depth for each beam. A position was calculated for the individual beam depths using AdMap (Mueller, 2007). AdMap was also used to interpolate positioning from the ADCP bottom track data under the bridge where GPS data were invalid. These techniques allow the ADCP to be used as a multibeam sonar with a sampling rate of approximately 1 Hz.

The bathymetry data from each survey were interpolated to a continuous grid around the cassion using kriging. Vertical changes in bed elevation between surveys were quantified using surface differencing (Figure 4). The elevations from the June survey were subtracted from those of the July survey. Positive values indicate fill and negative values indicate scour. For each new survey the previous surface was subtracted to document bed elevation changes through the summer. Scour was evident along the right-bank side of the caisson nose in June. This portion of the caisson is exposed to the highest velocities. The downstream left-bank side is on the lee side of the primary flow and was the highest elevation in June. In July, the scour hole at the nose of the caisson expanded to the left-bank side of the nose and down the length of the caisson's right-bank side. Scour at the nose was slightly greater in August when the bed elevation on the left-bank side of the pier nose was 0.8 m above the bottom of the caisson and the maximum flow depth was 14 m. The downstream left-bank side of the caisson scoured 2 m between the July and August measurements. Fill was measured around the entire pier in the October survey. Over 7 m of infilling occurred at the left-bank side of the caisson's nose between the August and October surveys. Elevations measured in October likely represent the full extent of fill because of the rapid decrease in both streamflow and sediment load in the fall. Bed elevations in October were compared to those surveyed in June and were higher in all areas except the downstream left-bank side of the caisson where the bed was 2 m lower than in June (Figure 4).

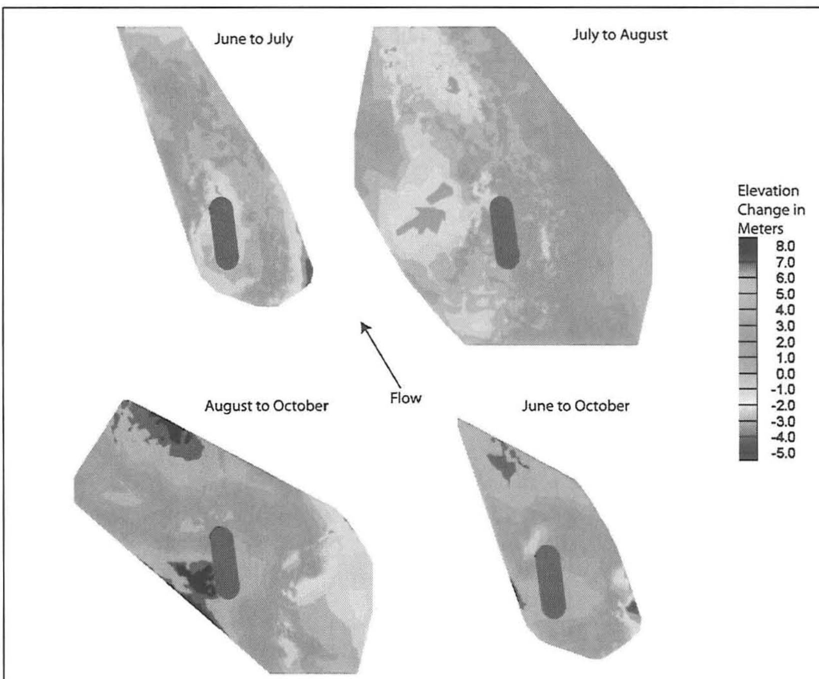

Figure 4: Plots of elevation change determined from surface differencing between surveys. Values were determined by subtracting the streambed elevations from the older survey from those of the newer. Warm colors indicate scour and cool colors indicate fill.

CONCLUSIONS

A multi-dimensional surface water model was used to evaluate the affects of two causeways in the Tanana River on streamflow hydraulics at bridge 505. This bridge is slated for replacement in 2010 because of age and streambed scour at a caisson that surrounds one of its piers. Results from four streamflow simulations did not indicate that streamflow hydraulics would be affected by the causeways located just 75 m downstream. Estimated pier scour computed from the results of the initial conditions scenario and the causeway scenario increased from 5.5 m to 5.6 m, respectively

Repeated multi-beam bathymetry surveys using an ADCP documented the dynamic nature of the streambed around the caisson. Positioning algorithms were used to accurately map thousands of bed elevation points under the bridge. These surveys tracked the streambed's response to a rising streamflow through the summer and into the fall recession. Scour was greatest along the nose and right-bank side of the caisson where flow approaches the bridge at an angle of 45 degrees. The minimum measured bed elevation in August was only 0.8 m above the bottom of the caisson. The scour hole filled as much as 7 m between August and October. The streambed likely fills to a similar elevation each fall as streamflow and sediment load decrease. This would indicate at least 7 m of scour since our observations were not continuous. The predicted scour for the caisson was 5.6 m for a 2-year recurrence interval flow. These findings are consistent with others from glacial-fed rivers in Alaska that experience seasonal bed fluctuations in excess of predicted scour for flood flows.

REFERENCES

Conaway, J.S., and Moran, E.H., 2004, Development and calibration of a two-dimensional hydrodynamic model of the Tanana River near Tok, Alaska: U.S. Geological Survey Open-File Report 2004-1225, 13 p.

Conaway, J.S., 2006, Temporal Variations of Scour and Fill Processes at Selected Bridge Sites in Alaska, in Proceedings of the Eight Federal Interagency Sedimentation Conference, April 2-6, 2006, Reno, NV, USA, 8 p.

Conaway, J.S., 2007, Analysis of Real-Time Streambed Scour Data from Bridges in Alaska: in Proceedings of the 2007 World Environmental and Water Resources Congress, May 15-19, 2007, Tampa, Florida, 11 p.

Heinrichs, T.A., Kennedy, B.W., Langley, D.E., and Burrows, R.L., 2001, Methodology and estimates of scour at selected bridge sites in Alaska: U.S. Geological Survey Water-Resources Investigations Report 00-4151, 44 p.

McDonald, R.R., Bennett, J.P., and Nelson, J.M., 2005, Multi-dimensional surface water modeling system user's guide: U.S. Geological Survey Techniques and Methods Report, book 6, section B, chap. 6, 156 p., accessed at http://wwwbrr.cr.usgs.gov/gstl/WebHelp_Pro/MD_SWMS.htm

Mueller, D.S., 2007, Acoustic Doppler Measurement Analysis and Processing (AdMap): U.S. Geological Survey National Surface Water Conference and Hydroacoustics Workshop, April 2-6, 2007, St. Louis, MO, USA.

U.S. Geological Survey, 1951-1954, Water resources data for Alaska, water years 1951-1954: U.S. Geological Survey Water-Data Report 51-1 to 54-1 (published annually)